UNIVERSITAT POLITÈCNICA DE VALÈNCIA

UNIVERSITAT POLITÈCNICA DE VALÈNCIA

Instituto Universitario Mixto de Biología Molecular y Celular de Plantas

Ingeniería metabólica de apocarotenoides del azafrán en frutos de tomate

Trabajo Fin de Máster

Máster Universitario en Biotecnología Molecular y Celular de Plantas

AUTOR/A: Gonzalez Aguilar, José Antonio

Tutor/a: Belles Albert, José María

Cotutor/a externo: GRANELL RICHART, ANTONIO

Director/a Experimental: LOBATO GOMEZ, MARIA

CURSO ACADÉMICO: 2023/2024

Abstract

Saffron (*Crocus sativus* L.) is cultivated for its multiple industrial and biological properties. The spice is obtained from the stigmata and is the most expensive in the world. The quality and characteristics of saffron depend on the content of crocetin, crocin, picrocrocin, and safranal. These are apocarotenoids, products derived from the metabolism of carotenoids, which are a class of secondary tetraterpenoid metabolites. Carotenoids have also been widely studied for their biological and commercial functions. This study aimed to explore a new pathway for producing these saffron apocarotenoids in tomato fruit (*Solanum lycopersicum*) by using the CCD4a from *Gardenia jasminoides*. This enzyme is responsible to produce the equivalent to saffron apocarotenoids in this specie. Several transgenic lines were generated carrying the *Gj*CCD4a in two different genetic backgrounds, MoneyMaker (MM) and a double mutant (*hp3/B*^{Sh}). Additionally, some lines also contained the *Cs*UGT91P3, implicated in the glycosylation of crocins. Thirteen lines were selected for in-depth analysis of targeted gene expression, as well as targeted metabolomic analysis. Crocins (and their precursor, crocetin) and picrocrocins were detected in all transgenic lines, reaching the highest accumulation (5.34 mg/g dry weight (DW)) in the *hp3/B*^{Sh} transgenic lines. This study supports the use of *Gj*CCD4a as a suitable biotechnological tool for producing saffron apocarotenoids in tomato.

Key words

Crocus sativus; *Gardenia jasminoides*; saffron; apocarotenoid; carotenoid; CCD; *Gj*CCD4a; *Cs*UGT91P3; metabolic engineering; tomato; lycopene; β-carotene; zeaxanthin; crocin; crocetin; picrocrocin.

Resumen

El azafrán (*Crocus sativus* L.) se cultiva por sus múltiples propiedades industriales y biológicas. La especia se obtiene de los estigmas y es la más cara del mundo. La calidad y las características del azafrán dependen de su contenido en crocetina, crocina, picrocrocina y safranal. Se trata de apocarotenoides, productos derivados del metabolismo de los carotenoides, que son una clase de metabolitos secundarios tetraterpenoides. Los carotenoides también se han estudiado ampliamente por sus funciones biológicas y comerciales. El objetivo de este estudio era explorar una nueva vía para producir estos apocarotenoides del azafrán en el fruto del tomate (*Solanum lycopersicum*) utilizando la CCD4a de *Gardenia jasminoides*. Esta enzima es la responsable de producir el equivalente a los apocarotenoides del azafrán en esta especie. Se generaron varias líneas transgénicas portadoras de la *Gj*CCD4a en dos fondos genéticos diferentes, MoneyMaker (MM) y un doble mutante (*hp3/B*^{Sh}). Además, algunas líneas también contenían el *Cs*UGT91P3, implicado en la glicosilación de las crocinas. Se seleccionaron trece líneas para analizar en profundidad la expresión de genes específicos, así como para realizar análisis metabolómicos específicos. Se detectaron crocinas (y su precursor, la crocetina) y picrocrocinas en todas las líneas transgénicas, alcanzando la mayor acumulación (5.34 mg/g de peso seco (DW)) en las líneas transgénicas *hp3/B*^{Sh}. Este estudio apoya el uso de *Gj*CCD4a como herramienta biotecnológica adecuada para producir apocarotenoides del azafrán en tomate.

Palabras clave

Crocus sativus; *Gardenia jasminoides*; azafrán; apocarotenoide; carotenoide; CCD; *Gj*CCD4a; *Cs*UGT91P3; ingeniería metabólica; tomate; licopeno; β-caroteno; zeaxantina; crocina; crocetina; picrocrocina.

Index

Introduction

Carotenoids

Carotenoids, a class of fat-soluble pigments known for their red, orange, and yellow colours, have been the subject of thorough examination due to their visual properties and health benefits. These compounds are synthesized by photosynthetic organisms, including cyanobacteria, algae, and plants, as well as certain fungi and bacteria [1]. They are classified into hydrocarbon carotenes with pure structures (α- and β-carotenes, lycopene) and oxygenated derivatives of xanthophylls (lutein, zeaxanthin, astaxanthin, fucoxanthin, cryptoxanthin, etc.) [2].

In green plant tissues, carotenoids play crucial roles in light capture, photoprotection, and the stabilization of photosynthesis. They also serve as secondary metabolites in flowers and fruits, attracting pollinators and aiding seed dispersal. Additionally, they serve as precursors to plant hormones and other apocarotenoids that influence development and responses to stress [3], [4].

Carotenoids have a high commercial value. They are the primary contributors to pigmentation in some ornamental plants and have applications in various industries such as pharmaceuticals, cosmetics, and food [5]. In humans, carotenoids are introduced to the organism through the diet. Carotenoids and their oxidative products exhibit various biological activities in humans, including the regulation of the cell cycle, cell differentiation, and modulation of growth factors. Additionally, these compounds play a role in preventing cardiovascular and metabolic diseases and cancer, among other health conditions. [6].

There are more than 700 carotenoids naturally produced, of which 40 are consumed in the human diet through fruits and vegetables. Major carotenoids found in human tissues are lycopene, β-carotene, β-cryptoxanthin, lutein, and zeaxanthin [6]. Lycopene is a red pigment which can be found naturally in plants such as tomato, watermelon, red and pink grape, or papaya [7]. It has been demonstrated to exhibit broad biological activity, including antifungal activity against *Candida albicans*. Additionally, it is implicated in mitigating the development of cardiovascular diseases, atherosclerosis, diabetes, and neurodegenerative diseases [5], [8]. β-carotene is an orange carotenoid, commonly referred to as pro-vitamin A, it is converted into vitamin A within the human body [9]. β-carotene is abundant in carrots, spinach, apricots, and mango, among other fruits and vegetables [7]. β-cryptoxanthin is a yellow carotenoid found in mango, papaya, and citrus such as orange and mandarin [7]. It has a role in lowering the risk of various types of cancer, including lung, stomach, and colon cancer, among others [2]. Lutein and zeaxanthin, both yellow xanthophylls, positively affect ocular diseases, safeguarding against oxidative damage in the retina [10], [11]. Some sources of lutein are watercress, spinach, and

broccoli. Lutein and zeaxanthin are present in maize, the latter is also accumulated in red pepper, mandarin, or wolfberry [7].

Carotenoid biosynthetic pathway

Carotenoids are terpenoids. The typical structure is formed by eight molecules of 5-C isopentenyl diphosphate (IPP) and its isomer dimethylallyl diphosphate (DMAPP) (40C). While this form is predominant in nature, shorter carotenoids (30C) as well as longer ones (45C and 50C) can also be found [1]. In plants, IPP and DMAPP are synthesized from two independent pathways: the cytosolic mevalonate (MVA) pathway and the plastidial 2-C-methyl-D-erythritol 4-phosphate (MEP) pathway. Although there is some evidence of exchange of these isoprenoid precursors between subcellular compartments, there must be a limitation in this transport, as plants in which the MEP pathway has been blocked cannot be rescued by precursors derived from MVA, and vice versa. MEP pathway is the primary route for synthesizing carotenoids in plants and other compounds such as chlorophylls, tocopherols, or gibberellins, among others [12]. The MEP pathway initiates with the condensation of a glyceraldehyde-3-phosphate molecule with a pyruvate, catalysed by the enzyme DXP synthase (DXS), considered the key regulatory enzyme in this pathway. Geranylgeranyl pyrophosphate (GGPP) is formed through the condensation of three units of IPP and one unit of DMAPP by the enzyme GGPP synthase [13]. GGPP serves as the universal precursor for carotenoid synthesis.

Carotenoid biosynthesis starts with the condensation of two GGPP molecules, forming 15-*cis*-phytoene. This crucial step is catalysed by phytoene synthase (PSY), serving as the primary limiting enzyme throughout the entire pathway [13]. While *Arabidopsis thaliana* possesses only one PSY, three PSY isoforms have been reported in tomato: PSY1, PSY2, and PSY3. The first two are primarily involved in the synthesis and accumulation of carotenoids in ripe fruits and green tissues, respectively. PSY3, on the other hand, is strongly expressed during the symbiotic interaction of mycorrhizae with roots, contributing to the formation of strigolactones [14]. The subsequent steps involve sequential desaturation reactions of 15-*cis*-phytoene catalysed by the enzymes phytoene desaturase (PDS), carotene isomerase (ZISO), and ζ-carotene desaturase (ZDS), leading to the synthesis of tetra-*cis*-lycopene (prolycopene). The latter is then converted into all-*trans*-lycopene, either by the enzyme carotenoid isomerase (CRTISO) in non-photosynthetic tissues or spontaneously in those tissues containing chlorophyll, induced by light [13], [15].

Then, lycopene is cyclated by lycopene ε-cyclase (LCY-E) and/or lycopene β-cyclase (LCY-B), resulting in the formation of α- and β-carotene, respectively. In tomato, two isoforms of LCY-B have been identified: LCY-B1 (also known as CRTL-B), which exhibits higher activity in green tissues and flowers, and LCY-B2 (also known as CYC-B), which is specific to chromoplasts [12]. In tomato, the hydroxylation

of α-carotene to lutein and β-carotene to zeaxanthin is done by four hydroxylases: two cytochrome P450 type hydroxylases (CYP97A and CYP97C) and two non-heme β-ring hydroxylases (BCH1 and BCH2). The transformation of zeaxanthin into violaxanthin is catalysed by zeaxanthin epoxidase (ZEP), and this process is reversed by violaxanthin de-epoxidase (VDE) [1], [13].

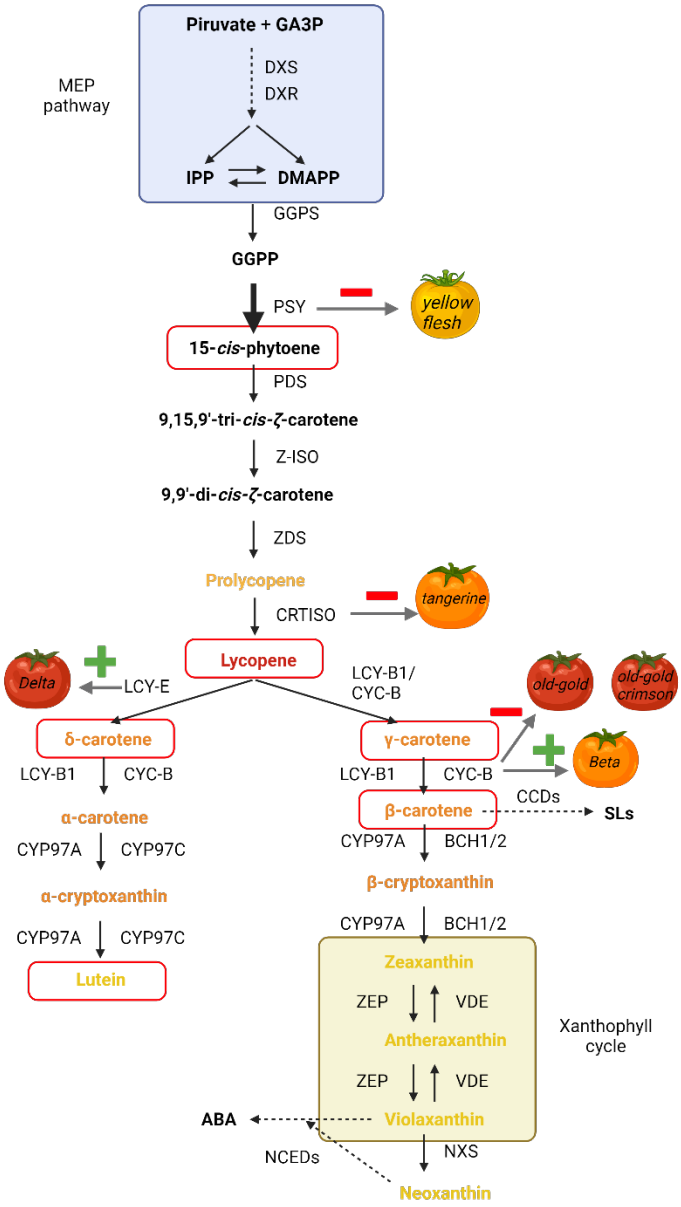

Figure 1. Overview diagram of carotenoid biosynthesis pathway in plastids and some colour-variants associated with mutant alleles of the biosynthetic genes in tomato. Main carotenoids accumulated in tomato fruit are in red boxes. MEP, methylerythritol 4-phosphate; GA3P, glyceraldehyde 3-phosphate; IPP, isopentenyl diphosphate; DMAPP, dimethylallyl diphosphate; GGPP, geranylgeranyl diphosphate; DXS, 1-deoxy-D-xylulose 5-phosphate (DXP) synthase; DXR, DXP reductoisomerase; GGPS, GGPP synthase; PSY, phytoene synthase; PDS, phytoene desaturase; Z-ISO, ζ-carotene isomerase; ZDS, ζ-carotene desaturase; CRTISO, carotenoid isomerase; LCY-E, lycopene ε-cyclase; LCY-B, lycopene β-cyclase; BCH, β-carotene hydroxylase; CYP97A, cytochrome P450 carotene β-hydroxylase; CYP97C, cytochrome P450 carotene ε-hydroxylase;

ZEP, zeaxanthin epoxidase; VDE, violaxanthin de-epoxidase; NXS, neoxanthin synthase; CCD, carotenoid cleavage dioxygenase; NCED, 9-*cis*-epoxycarotenoid dioxygenase. Adapted from [2], [12], [13], [16].

Modification of tomato carotenoid composition by genetic approaches

Carotenoids are highly produced in tomatoes, and more than 20 carotenoids have been identified in tomatoes and tomato-based products. The distribution of carotenoids in tomato fruits is not uniform, and the composition is greatly influenced by factors such as the cultivar (genotype), ripeness level, climate, environmental conditions, and cultivation methods. In the ripe fruit, the major carotenoids in most red ripe tomatoes are lycopene (≈90%), β-carotene (≈5–10%), and lutein (<1%) [17].

Over the years, several natural mutations that alter the carotenoid biosynthesis pathway in tomato fruit have been reported, some described below [16].

PSY1 is a crucial step in carotenogenesis and is the first enzyme involved. Two recessive mutations in the locus *r* give an atypical *yellow flesh* colour tomato. These mutations are responsible for a non-functional PSY1, resulting in a lack of phytoene and lycopene [16]. Alternatively, transgenic tomato lines overexpressing *SlPSY1* translated into a total carotenoid increase in red fruits. The predominant carotenoids responsible for these increases were phytoene (1.5- to 3.0-fold), lycopene (up to 1.5-fold), and β-carotene (1.5- to 3.0-fold) relative to WT [18]. In contrast, [18]

On the other hand, mutations in enzymes involved in the latter steps of carotenoid biosynthesis had a major influence on the carotenoid composition in tomato fruits [16]. Two allelic mutations of CRTISO were first identified in the *tangerine* mutant with an orange flesh colour due to prolycopene accumulation in place of lycopene. These mutations result in the absence of a functional enzyme [19].

LCY-E expression decreases during the fruit ripening. In contrast, this expression is radically increased in the Delta mutant, leading to an accumulation of δ-carotene and lutein. Although the amino acid sequence is almost identical in the *Delta* mutant and the wild type lines, the variation found upstream of the promoter region could explain this difference in expression levels [16].

Mutations in the CYC-B enzyme have been also studied. Three alleles of CYC-B were reported, named *Beta* (B^{Sh}), *old-gold* (*og*) and *old-gold crimson* (og^{c}) [20]. The first one was introduced in cultivated tomato by introgression from wild *S. habrochaites* [21]. *Beta* is responsible for the orange colour in the fully ripened fruit because of the accumulation of β-carotene at the expense of lycopene. This is provoked by the increase in the expression of CYC-B [22], [23]. Conversely, *og* and og^{c} are null mutations of the same enzyme that cause a lack of β-carotene in the ripe fruit [24].

Another mutation, *high-pigment 3* (*hp3*), resulted in mutants with a defective ZEP [23]. This mutation causes a deficiency in ABA levels. Morphologically, the number and the compartment size of plastids

have been increased in *hp3* mutants. The effects of this are an increase in the carotenoid biosynthesis and larger compartments to store them, resulting in tomatoes with higher carotenoid levels [25]. Another high-pigmented mutation is *hp2g*^{dg}. This consists of the recessive mutation *hp2* in the DE-ETIOLATED 1 (DET1) gene, giving photomorphogenic mutants. The *hp2dg* mutants showed darker pigmentation of leaves and fruits, the latter due to significantly increased levels of chlorophylls in immature green fruits and carotenoids, mainly lycopene, in red ripe fruits. [26].

There are many studies that aim to alter the carotenoid profile of tomato fruit. However, the highest levels of zeaxanthin, the precursor used by all CCDs that produce saffron apocarotenoids, were achieved by combining *B*^{Sh}, *hp3, hp2*^{dg}, and *GREEN-STRIPE* (*gs*) mutations. The quadruple mutated tomato plant was named Xantomato, zeaxanthin and β-carotene are their main carotenoids in fruit [11] (Figure 2). Xantomato is the most suitable platform to produce saffron apocarotenoids in tomato by introducing any of the CCDs that have been discovered in different plant species (Lobato M, unpublished results); however, the combination of the four mutations has pleiotropic effects on plant growth. The intermediate mutants obtained in this study have high β-carotene content and lower zeaxanthin levels with lower pleiotropic effects [11], and they can be used to produce saffron apocarotenoids by introducing the CCD from *Gardenia jasminoides*, which can also use β-carotene as substrate [27].

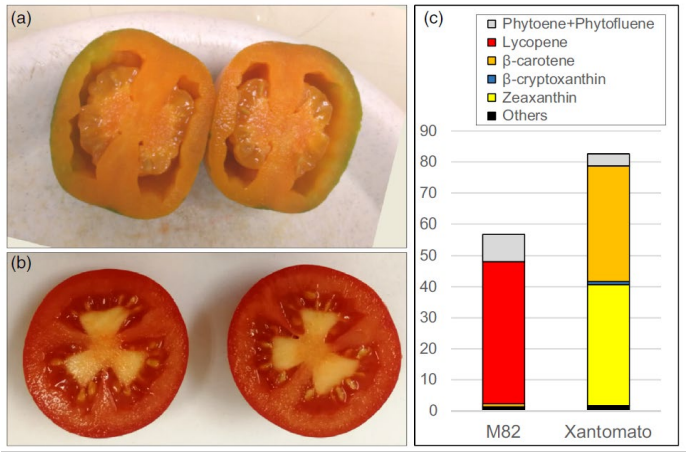

Figure 2. a) Typical aspect of Xantomato fruits; b) fruit aspect of the variety M82; c) carotenoid composition of Xantomato and M82 (WT) fruits (µg/g FW). FW, fresh weight. Extracted from [23].

Apocarotenoids

Apocarotenoids are oxidative products of carotenoids, which can occur through two mechanisms: non-enzymatic nonspecific oxidation induced by reactive oxygen species and enzymatic oxidation. The latter can be non-site specific, conducted by lipoxygenases and peroxidases, or site-specific, catalysed by a family of enzymes known as carotenoid cleavage dioxygenases (CCDs). Apocarotenoids constitute a broad and diverse group of compounds that play crucial roles in plant metabolism. They contribute

to regulate plant growth and development, participate in the synthesis of phytohormones like abscisic acid (ABA) and strigolactones (SLs), and respond to both abiotic and biotic stresses. Additionally, they hold commercial significance as products such as food additives, colorants, and pharmaceuticals [13], [28], [29].

Within the CCD family, two big subfamilies emerge. The first is constituted by 9-*cis*-epoxy-carotenoid-dioxygenases (NCEDs), responsible for catalysing the reaction that cleaves 9-*cis*-violaxanthin and 9-*cis*-neoxanthin to produce xanthoxin, the precursor of abscisic acid (ABA). The first NCED, named VP14, was discovered in maize. Subsequently, up to five distinct NCEDs have been identified in *Arabidopsis* as participants in ABA synthesis: NCED1, NCED2, NCED3, NCED6, and NCED9 [30] (Figure 2).

The other major enzyme family is the CCDs, exhibiting in general a higher degree of promiscuity compared to the NCEDs. These CCDs have been categorized into six subfamilies—CCD1, CCD2, CCD4, CCD7, CCD8, and the recently discovered ZAS (zaxinone synthase) and CCD10—based on substrate specificity and cleavage site characteristics [13], [29]. CCD1 enzymes, found in the cytosol, exhibit a wide substrate specificity. They cleave symmetrically various carotenoid, including lycopene, β-carotene, lutein, and zeaxanthin at the C9-C10 (C9'-C10') positions, resulting in the production of dialdehydes and ketones. Moreover, these enzymes can cleave apocarotenoids such as β-apo-8'-carotenal and β-apo-10'-carotenal [28]. CCD2 enzymes, closely linked to CCD1, are located within plastids. Originally identified in *Crocus sativus*, these enzymes cleave zeaxanthin at both C7–C8/C7'–C8' sites, yielding crocetin dialdehyde as a precursor to subsequent crocetin and crocin formation [29]. CCD4 enzymes are located within the plastids, with their classification based on their substrate specificity and the double bonds they cleave. Some CCD4 enzymes target the C9'-C10' and/or C9–C10 double bonds in β-carotene or β-apo-8'-carotenal, resulting in the production of β-ionone. Others demonstrate specificity for the double bond at position 7,8, leading to the asymmetric cleavage of β-cryptoxanthin and zeaxanthin at the 7,8/7'–8' positions, yielding β-citraurin and apo-80 -β-carotenal [31]. In SL biosynthesis, CCD7 and CCD8 have distinctive functions in a sequential manner. CCD7 catalyses the cleavage of 9-*cis*-β-carotene, yielding 9-*cis*-β-apo-10'-carotenal, subsequently processed by CCD8 to produce carlactone [32]. Zaxinone synthase (ZAS) operates by cleaving zeaxanthin and derivates at the specific C13/C14 double bond, producing zaxinone. This molecular entity assumes a regulatory function in orchestrating plant growth dynamics and concurrently modulates the biosynthesis pathways of SL and ABA [2], [32]. Finally, CCD10, identified in *Nicotiana tabacum*, cleaves carotenoids at both the C9–C10 (C9'–C10') and C5–C6 (C5'–C6') positions [33].

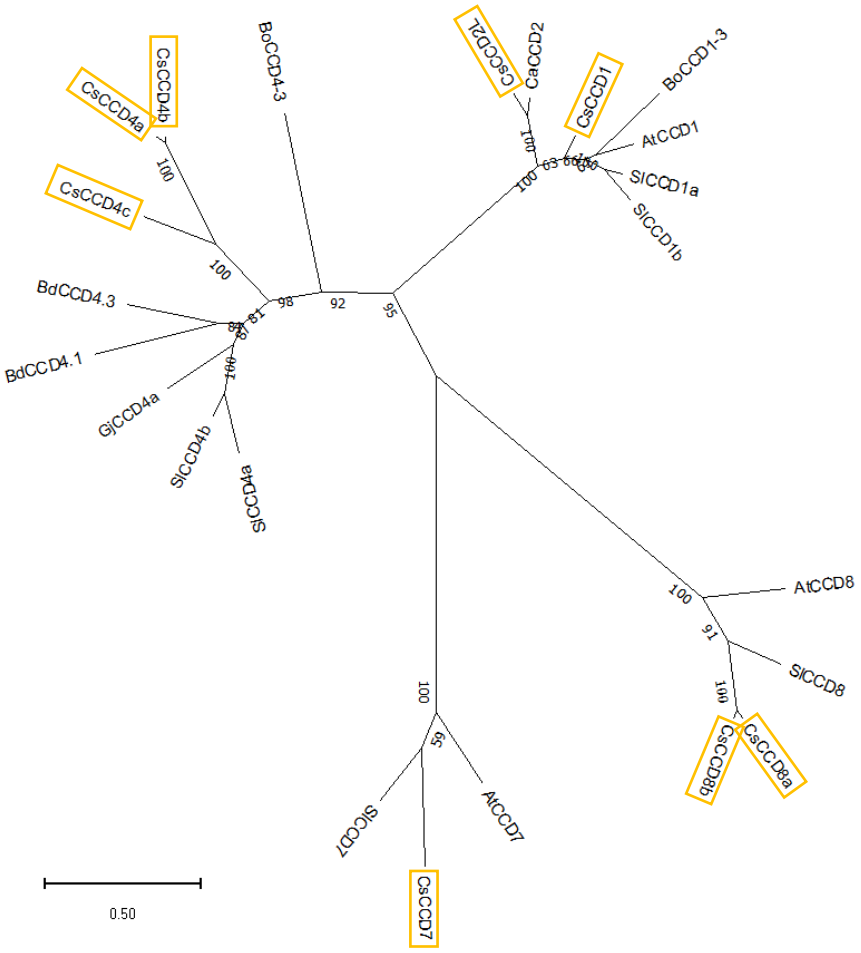

Figure 3. Phylogenetic analysis of CCD from some plants. The evolutionary history was inferred by using the Maximum Likelihood method and JTT matrix-based model. The tree with the highest log likelihood is shown. This analysis involved 23 amino acid sequences. CCDs from *C. sativus* are indicated with yellow boxes. The accession number are shown in the Supplementary Material Table 1. *Bo*, *Bixa Orellana; Bd*, *Buddleja davidii*; *At*, *Arabidopsis thaliana*; *Ca*, *Crocus ancyrensis*; *Sl*, *Solanum lycopersicum*; *Gj*, *Gardenia jasminoides.* Phylogenetic analysis was performed with MEGA11 (https://megasoftware.net/) [34].

Saffron apocarotenoids

Saffron (*C. sativus L.*) is a sterile, perennial triploid plant that reproduces vegetatively due to the presence of sterile flowers. Renowned as the world's most expensive spice, saffron is derived from the dried stigmas of its flowers. It stands out for its distinctive physicochemical attributes, including colour, flavour, aroma, and biological properties. [35]. The unique properties of saffron make it versatile across various domains. Throughout history, it has served as a food additive and found application as a dye in the textile and cosmetic industries, with a significant role in pharmaceuticals. Saffron has documented medicinal uses for treating health conditions such as Alzheimer's, diabetes, cancer, impotence, and fatty liver disease [36], [37]. The organoleptic and biological properties of saffron are primarily due to the accumulation of its three main apocarotenoids: crocins, picrocrocin, and safranal.

These metabolites contribute to the colour, taste, and aroma of the stigmas [36], their biosynthesis is represented on Figure 4.

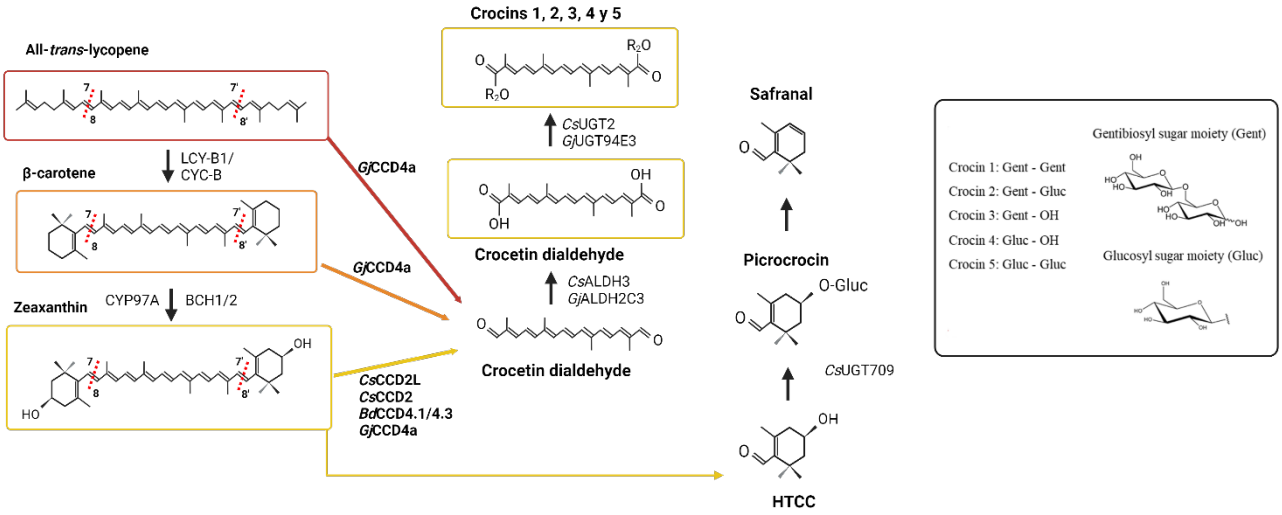

Figure 4. Saffron apocarotenoid biosynthesis pathway. Enzymes that naturally produce saffron apocarotenoids are included. Adapted from [38].

Crocetin and its esters, crocins, are responsible for the red coloration of saffron and the yellow colour in aqueous solutions [37]. In the stigmata of *C. sativus*, the biosynthesis of saffron apocarotenoids initiates with the cleavage of zeaxanthin by *Cs*CCD2, resulting in a crocetin dialdehyde molecule and two molecules of 4-hydroxy-2,6,6-trimethyl-1-cyclohexene-1-carboxaldehyde (HTCC) [39], [40]. Crocetin dialdehyde is highly reactive and undergoes conversion to crocetin by *Cs*ALDH. The final stage of this process involves a series of successive glycosylations, yielding crocins with varying degrees of glycosylation, which are stored in the vacuole. The addition of glucose and gentiobiose residues is crucial for the stability, localization, and chemical properties of the compounds. These glycosylations are catalysed by UDP-glucose-dependent glycosyltransferases (UGTs), widely found in plants [41]. There are two types of UGTs: those generating crocetin monoglucosyl and diglucosyl esters, such as *Cs*UGT2; and those responsible for secondary glycosylation on glucose residues, which could add a glucosyl, glucuronosyl, xylose, rhamnosyl, or galactosyl molecule to an existing sugar moiety in different metabolites, resulting in the formation of gentiobiose groups [36], [39], [41]. *Cs*UGT709 converts HTCC molecules into picrocrocin, a compound further metabolized to produce safranal [40].

Metabolic engineering of crocins

As mentioned earlier, saffron, also recognized as red gold, stands out as a highly valuable and costly spice to procure. The labour-intensive process involves the processing of approximately eighty kilograms of flowers to yield 1 kilogram of saffron, equating to a demanding 370-470 hours of labour.

Its production is predominantly concentrated in Iran, commanding a staggering 95% of the global annual output. Spain, Greece, Italy, and India contribute as minor producers in this industry [35], [37].

Saffron is not exclusively produced by *C. sativus*; other plants, such as *Gardenia jasminoides* and *Buddleja davidii,* have been identified to naturally produce saffron. These plants feature CCD4 enzymes, *Gj*CCD4a, *Bd*CCD4.1, and *Bd*CCD4.3, known for their activity in the synthesis of crocins. All mentioned CCDs use zeaxanthin as a substrate to produce crocins. Furthermore, *Gj*CCD4a can also use lycopene and β-carotene as substrates [42].

A new source of crocins and biotechnological tools for their production has recently been reported and corresponds to the CCDs of two species of *Verbascum*, *V. giganteum* and *V. sinuatum*. These CCDs are CCD1, CCD4.1, CCD4.2 and CCD4.3. In *Verbascum* sp., saffron apocarotenoid accumulation occurs in the flowers, and the profile of compounds is similar to that found in *Buddleja davidii*. Precisely, CCD4.1 and CCCD4.3 of the two *Verbascum* species show more homology with *Bd*CCD4.1, and *Bd*CCD4.3, than with the rest of the reported CCD4. [43].

Overall, understanding the enzymes involved in saffron apocarotenoid biosynthesis has been crucial for effective metabolic engineering in both plants (Table 1) and microorganisms [44].

Table 1. Plant heterologous platforms for saffron apocarotenoids production. DW: Dry Weight; *Zm: Zea mays*; *Pa: Pantoea ananatis*; tp: transit peptide; *Os: Oryza sativa; Vg, Verbascum giganteum.*

Plants	**Gene(s) introduced**	**Crocin + crocetin + picrocrocin production**	**Reference**
N. benthamiana	*CsCCD2L*	2.18 mg/g DW	[45]
	BdCCD4.1	No quantified	[45]
	VgCCD4.1	1.78 mg/g DW	[43]
N. tabacum	*CsCCD2L*	136 µg/g DW	[40]
N. glauca	*CsCCD2L*	400 µg/g DW	[40]
Oryza sativa	*CaCCD2, AtDXS, ZmPSY1, and PaCrtI*	0.022 µg/g	[29]
S. lycopersicum	*CsCCD2L*	16.9 mg/g DW	[46]
S. tuberosum	*CsCCD2L, UGT74AD1, UGT709G1*	1.16 mg/g DW	[47]
Citrus paradisi calli	*CsCCD2L, tpCrtB, OsBCH*	9.88 µg/g DW (only crocetin)	[27]
	GjCCD4a, tpCrtB, OsBCH	2.96 µg/g DW (only crocetin)	[27]

The production of crocins and picrocrocins has been achieved in *Nicotiana benthamiana* leaves by transiently expressing different CCDs, such as *Cs*CCD2L, *Bd*CCD4.1 and *Vg*CCD4.1. *Vg*CCD4.1 was chosen to be expressed in heterologous systems to obtain crocins because it had the highest expression level of all CCDs mentioned above [43], [45]. Recent investigations have successfully used stable transformation to produce crocins in alternative *Nicotiana* species, *N. glauca* and *N. tabacum*. Both species exhibited a consistent crocin accumulation pattern by the expression of *Cs*CCD2L, mirroring the characteristics observed in *N. benthamiana*. Nevertheless, the quantity of crocins produced by stable systems is considerably diminished in contrast to transient expression. Notably, *N. glauca* (400 μg/g DW) exhibited superior crocin accumulation compared to *N. tabacum* (136 μg/g DW), though both accumulated significantly lower levels compared to transient *N. benthamiana* (2 mg/g DW) [40]. The expression of *Crocus ancyrensis CCD2* in rice callus in conjunction with *AtDXS*, *ZmPSY1*, and *PaCrtI*, resulted in the successful accumulation of crocetin at a concentration of 0.022 μg/g [29]. Up to the moment, the most efficient system for apocarotenoid production is Tomaffron, which consist of transgenic tomato plants that express *Cs*CCD2L with the control of the E8 fruit-specific promoter. The accumulation of crocins and picrocrocin was of 14.48 mg/g DW and 2.42 mg/g DW, respectively. Tomaffron was obtained from *S. lycopersicum* cv. MM, the ripe fruits from this cultivar accumulate high levels of lycopene, lower levels of β-carotene, very low levels of lutein, and undetectable levels of zeaxanthin. In Tomaffron, lutein was not detected either, demonstrating that *Cs*CCD2L can also use lutein as a substrate to produce crocins [46].

The aim of this thesis is to obtain an alternative method for producing crocins in tomato fruit by using *Gj*CCD4a instead of *Cs*CCD2 and using a mutant tomato cultivar that accumulates zeaxanthin and β-carotene in the fruit instead of lycopene. In addition, the effect of *Cs*UGT93P1 on crocin accumulation will be evaluated.

Objectives

- Design gene constructs with diverse gene combinations to engineer saffron apocarotenoid biosynthesis in tomato fruit.
- Transform tomato with these constructions and regenerate transgenic tomato plants.
- Assess the expression patterns of the transgenes and the carotenoid biosynthetic pathway genes in the transgenic tomato plants.
- Evaluate saffron apocarotenoid accumulation in fruit of the different transgenic plants.

Materials and methods

GoldenBraid Cloning Strategy

To construct the DNA elements utilized in this thesis, the GoldenBraid (GB) cloning system was employed. This system follows a standardized approach for assembling distinct DNA parts (level 0) within the same functional category (e.g., promoters, CDS, or terminators), resulting in the formation of transcriptional units (TUs) (level 1). The process involves the design of specific overhangs for each category, utilizing type IIS restriction enzymes, which cleave DNA a few nucleotides away from their recognition sites, allowing for custom definition. Once transcriptional units are assembled, the GB system facilitates the creation of modules by integrating these units, leading to the development of modules, which consist of multigene constructs (level >1) [48].

The products of the GB reactions were transformed into *E. coli* Mix & Go competent cells for plasmid propagation, following the Mix & Go *E. coli* Transformation Kit Protocol (ZYMO RESEARCH, Freiburg, Alemania). A total of 5 µl of the ligation product was gently mixed with 50 µl of competent cells and incubated on ice for 5 minutes. Subsequently, 500 µl of SOC medium were added. After one hour of shaking at 37ºC, transformed cells were plated onto LB agar plates containing the appropriate antibiotic (chloramphenicol, kanamycin, or spectinomycin at 50 mg/L, in pUPD2, pDGB3alpha, or pDGB3omega, respectively), 40 mg/L X-gal, and 0.4 mM IPGT for blue/white colony screening.

Isolated white colonies were cultured overnight in 4 ml of LB culture media containing the appropriate antibiotic. Subsequently, plasmid DNA isolation was performed using E.Z.N.A. Plasmid Mini Kit I (Omega Bio-Tek, Norcross, Georgia) from a 3 ml *E. coli* culture, following manufacturer's instructions. To confirm the correctness of the product, a 1-hour restriction reaction at 37ºC was conducted, selecting the restriction enzyme to obtain a clear band pattern that allows the differentiation of our construct from the empty destination vector, followed by electrophoresis on a 1% agarose gel stained with ethidium bromide to analyse the resulting band patterns. In the level 0 constructions, the sequences were sequenced as an additional verification step after obtaining the correct band pattern in the restriction enzyme reaction. Details of all plasmids generated in this project are provided in the Supplementary Material.

GoldenBraid domestication

The gene CDSs utilized in this study were generated using the domestication strategy outlined by A. Sarrion-Perdigones et al. (2013). *GjCCD4a* CDS sequence [27] was entered in the GB Domesticator tool, which returned a domesticated sequence. The domestication process involves BsaI and BsmBI internal sites removal and the addition of the appropriate 4-nt flanking overhangs according to the GB grammar. The sequence given by GB Domesticator tool was ordered in a gBlock (IDT, Coralville, US).

To create the DNA part corresponding to level 0, the multipartite restriction-ligation reactions aimed at cloning *GjCCD4a* into the domesticator vector pUPD2; the final volume of the reaction was 15 µl. The reaction included 60 fmol (20 fmol in case it is not a linear DNA sequence), each of *GjCCD4a*, and 20 fmol of pUPD2. Additionally, 5-10 units of BsmbI restriction enzyme and 3 units of T4 ligase were incorporated. T4 ligase buffer at 1X concentration and Bovine Serum Albumin (BSA) at 1X were added to create an optimal environment for the activity of both enzymes. This reaction underwent 40 digestion/ligation cycles, comprising 2 minutes at 37ºC and 5 minutes at 16ºC. *CsUGT93P1* CDS in pUPD2 was kindly provided by Dr. Lourdes Gómez-Gómez from UCLM.

The remaining DNA components utilized in this study had previously undergone domestication and were available at the GB database. Detailed information about these components can be found in the Supplementary Material Table 1. The *E. coli* glycerol stocks needed for this project and stored in the GB repository, were refreshed in liquid LB supplemented with the corresponding antibiotic.

Transcriptional units (TU) and Binary assembly

To generate level 1 and levels >1 constructs from GB parts (level 0), subsequent GB reactions were carried out by mixing each DNA element to be assembled, the destination vector pDGB3 (alpha1/2 or omega1/2), the respective type IIS enzyme (BsmBI or BsaI for omega or alpha destination vectors, respectively), and T4 ligase, T4 ligase buffer, and BSA. Reactions were optimized by adding each DNA part in equimolar amounts (20 fmol each) and establishing a reaction volume of 15 µl. Incubation of reactions occurred as explained above. The level 1 and level >1 constructs are showed in Figure 5.

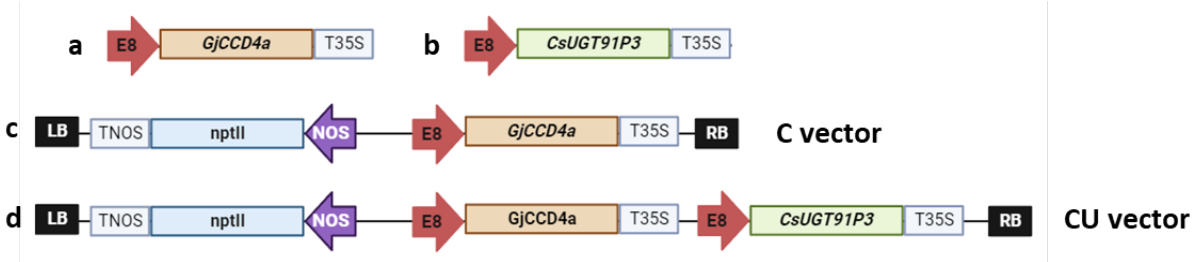

Figure 5. GB constructions generated. a) and b), level 1 constructions; c) and d) level >1 constructions (C, *E8:GjCCD4a*; CU, *E8:GjCCD4a_E8:GjCCD4a*). E8, tomato fruit-specific promoter; T35S, Cauliflower Mosaic Virus (CaMV) 35S terminator; NOS, nopaline synthase promoter; TNOS, nopaline synthase terminator, RB, right border; LB, left border.

Agrobacterium transformation

After the verification of the C and CU vectors on *E. coli*, *Agrobacterium tumefaciens* LBA4404 was transformed with them.

100-200 ng of purified DNA plasmid were mixed with 50 µl competent cells and transferred to an electroporation cuvette. Then, a 1.44 kV/cm pulse was applied followed by adding 500 µl of SOC medium (Supplementary Material 4) for cell recovery. The cell suspension was then grown at 28ºC in

continuous shaking for 2 h, and 50 µl of bacteria culture were plated onto LB agar containing rifampicin (*A. tumefaciens* LBA4404 has rifampicin resistance) and the corresponding antibiotic.

The plates were incubated for three days at 28ºC, and the resulting colonies were grown into 5 ml of LB culture media containing rifampicin and the corresponding antibiotic. Plasmid DNA isolation from *Agrobacterium* was conducted using QIAPrep Spin Miniprep Kit (QIAGEN, Hilden, Germany). Subsequently, the isolated plasmids underwent verification through restriction assays, following the previously described procedure.

Plant Material

Two different tomato cultivars were used to perform the transformations: *S. lycopersicum* cv. Moneymaker (MM), which accumulates high levels of lycopene in the fruit, and the tomato double mutant line *hp3/B*^{Sh}, which accumulates high levels of β-carotene and detectable levels of zeaxanthin in the fruit [11].

Transgenic T0 plants were grown in the greenhouse. Tomato fruits were collected at three different stages, mature green stage (when the fruit had reached its maximum size but did not reach the breaker stage); 5 days after breaker (Br+5), and 10 days after breaker (Br+10). For sample collection, the pericarp was separated from the seeds, cut into pieces, and immediately frozen in liquid nitrogen. For each plant, a pool of pericarps from three to five tomatoes was ground in liquid nitrogen, freeze-dried, and stored at -80 ºC for carotenoid, apocarotenoid, and RNA analyses.

Tomato transformation

For tomato transformation, the procedure described by Ellul et al. (2003) was followed. All tomato transformation media are listed on the Supplementary Material Table 5. For each transformation event, approximately 50 seeds were sterilized with 50% bleach and one drop of Tween 20 for 30 minutes. Then, seeds were washed with autoclaved distilled water at least three times. Sterile seeds were placed on germination media (GM) at 24°C in darkness for 3 days and then transferred to light for 5 days.

Two days prior to tomato transformation, the agrobacteria culture with the construct of interest was grown in MGL media (Supplementary Material Table 4) supplemented with the corresponding antibiotic at 28ºC. On the transformation day, the agrobacteria culture was initiated by adding 1 mL of the saturated preculture to 50 ml of TY media (Supplementary Material Table 4) for each construction. A total of 100 µL of acetosyringone 100 mM were added to induce the agrobacteria. The flasks were placed at 25ºC without light and shaking.

The OD600 of the agrobacteria was adjusted to 0.1. Then, plant explants were cut in the agrobacteria culture, incubated for 20 minutes, and placed on co-cultivation media. Co-cultivation occurred for 2 days at 24ºC in the dark. Then, the explants were transferred to induction media 1 (IM-1) for 10 days, and then to IM-2 every 21 days. Timentin was removed from IM-2 after three transfers.

Once the shoots appeared, explants were transferred to elongation media (EM) for them to elongate or directly cut and placed on rooting media (RM). Shoots were kept on RM until they developed roots; then they were transferred to the greenhouse and genotyped. The transformation procedure is summarised in Figure 6.

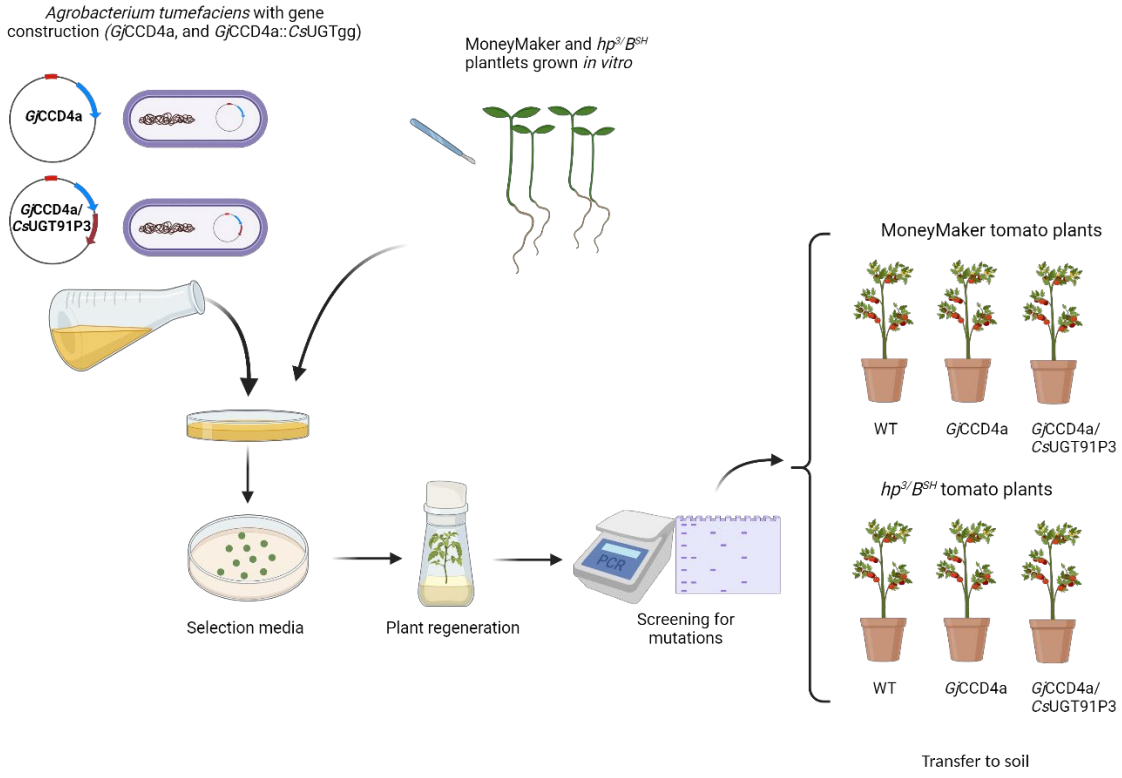

Figure 6. Tomato transformation process.

Genomic DNA extraction

Genomic DNA extraction was performed to genotype the putative transgenic lines. One or two small leaves from each plant were frozen in liquid nitrogen. The frozen sample underwent grinding using a Mixer Mill MM400 (Retsch Haan, Nordrhein-Westfalen, Germany) for 30 seconds at 30 Hz. Subsequently, 600 µl of CTAB buffer were added (Supplementary Table 5) and the mixture was incubated at 65 ºC for 45 minutes.

Subsequently, 600 µl of chloroform:isoamylalcohol (24:1) were added, and the mixture was vortexed and then centrifuged at 13,000 rpm for 15 minutes. The upper phase was carefully transferred to a

new tube. One volume of cold isopropanol was added, and the mixture was inverted for the DNA to precipitate. The mixture was kept on ice for 20 minutes, and then centrifugated at 13,000 rpm for 10 minutes. The resulting pellet was washed with 600 µl of ice-cold 80% ethanol, followed by centrifugation at 13,000 rpm for 5 minutes. The supernatant was discarded, and the pellet was air-dried. Finally, the pellet was reconstituted in 50 µl of Milli-Q water, incubated for approximately 30 minutes at 4ºC, vortexed, and the DNA concentration and quality were assessed using a NanoDrop Spectrophotometer.

PCR amplification

The extracted gDNA was used for *Gj*CCD4a and *Cs*UGT91P3 amplification by PCR. The amplification was carried out following the MyTaq DNA Polymerase (Bioline, Colchester, England) protocol. The PCR reaction setup and cycling conditions were executed following the manufacturer's instructions, with a final volume of 15 µl. Primers used are listed in Supplementary Material Table 3.

Measurement of fruit color

The tomato skin color was also measured at three diametrically opposite spots at the equatorial of the fruit using a colorimeter (Minolta CR-400, Minolta, Osaka, Japan). The calibration was performed following the manufacturer's standard white plate. Color changes were quantified in the XYZ* color space. Lately, the variables to determine color spaces CIE L*C*h, y CIE L*a*b* were calculated. L* refers to lightness, ranging from 0= black to 100= white; hue angle (H*) value is defined as a color wheel, with red-purple color at an angle of 0°, yellow color at 90°, bluish-green color at 180° and blue color at 270°, and chroma (C*) represents color saturation, which varies from dull (low values) to vivid (high values). In CIE Lab*, a* determines the red-green color (+ red color, - green color); and b* defines the yellow-blue color (+ yellow color, - blue color) [50].

Gene expression analysis

Lyophilized material was used for RNA isolation with the GeneJET Plant RNA Purification Mini Kit (Thermo Fisher Scientific). The RNA was quantified using a NanoDrop Spectrophotometer. To achieve this, total RNA underwent treatment with Recombinant DNase I (RNase-free) (Takara), following the manufacturer's instructions.

cDNA was synthesized using the PrimeScript™ RT-PCR Kit (Takara). The cDNA was diluted at 1/25 to perform the qPCR reactions. The qPCR reactions were done with the TB SYBR Premix Ex Taq (Takara) following the manufacturer's instructions. The qPCR reactions were done using the Applied Biosystems 7500 Fast Real-Time PCR System. *Sl*actin2 gene was used as internal housekeeping gene. Three technical replicates were used for each sample and gene were done. Data processing was done using

the ΔΔCt method (Livak & Schmittgen, 2001). Primers used for RT-qPCR reactions are listed in Supplementary Material Table 3.

Crocin and picrocrocin analysis

Crocins and picrocrocin were extracted and analysed as previously described by Demurtas et al. (2023) with some modifications. 10 mg of lyophilized tomato fruit were weighed. 800 µl of 75% (*v/v*) methanol spiked with 0.1% formic acid (with 0.5 ug/ml Formononetin as internal standard) was added to 10 mg of freeze-dried tomato sample with vigorous agitation for two rounds of 20 minutes, keeping the samples during 5 minutes at room temperature. Samples were then centrifuged at 14,000 rpm for 15 minutes; the supernatant was collected, filtered with HPLC PTFE filter tubes (0.22 µm pore size), and subjected to high performance liquid chromatography-photodiode array detection-high resolution mass spectrometry (LC–PDA–HRMS) analysis using a Q-Exactive mass spectrometer (Thermo Fisher Scientific) [51].

Statistical analysis

The statistical test analysis was performed in R and the test used were t-test, ANOVA, Tuckey, used depending on the nature of the data. The packages used in R were *tidyverse*, *dplyr*, *rstatix*, *ggstatsplot* and *agricolae*.

Results

Generation of Transgenic Plants containing *GjCCD4a* and *CsUGT91P3*

Tomato (cv. MM and *hp3/B*^{Sh}) was transformed with two vectors (C and CU). A total of 15 transgenic lines were confirmed by PCR analysis and then transferred to soil. Among these fifteen lines, 11 are in the MM background. Within the MM group, a total of seven lines (#3, #30, #31, #32, #33, #34, and #35) contained *GjCCD4a*, and four lines (#21, #23, #25, and #27) contained both *GjCCD4a* and *CsUGT91P3*. Four transgenic lines were obtained from the double mutant *hp3/B*^{Sh} background, where three (#1, #3, and #12) contained only *GjCCD4a*, and one line (#15) contained both *GjCCD4a* and *CsUGT91P3*.

Analysis of fruit color

The initial assessment conducted to determine if the transgenic lines were expressing the genes and, consequently, accumulating crocins, involved examining the fruit color. Crocins contribute to yellow color, so the fruits were expected to lose the intense red color caused by high lycopene accumulation (in MM lines) and take on a more yellow-orange hue. In the *hp3/B*^{Sh} lines, visual inspection is more challenging since, due to the accumulation of β-carotene, the fruits already exhibit orange-colored fruits. Figure 7 illustrates transgenic tomatoes from MM and *hp3/B*^{Sh} lines. Some MM fruits with both transgenes displayed a less intense color. In the *hp3/B*^{Sh} fruits, this difference between constructions could not be easily discerned by the naked eye.

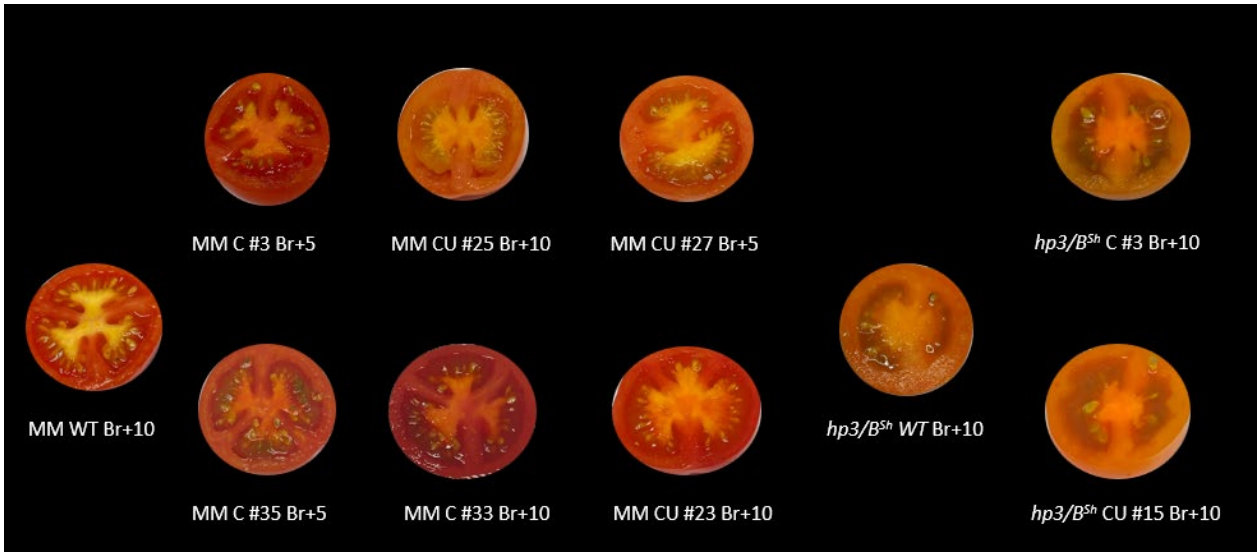

Figure 7. Transgenic tomato fruits of some lines at fruits at breaker after 5 days (br+5) and at breaker after 10 days (br+10). C, *GjCCD4a*; CU, *GjCCD4a-CsUGT91P3*.

To measure the color, a colorimeter was utilized, allowing the quantification of each fruit's color based on parameters such as CIE LCH and CIE Lab*. These variables were calculated, and a principal components analysis (PCA) was performed. The results were depicted in a biplot (Figure 8) to ascertain whether there was any separation among transgenic lines and WT.

In Figure 8a, all br+10 fruits are represented, colored by background: MM or *hp3/B^{Sh}*. Between both dimensions, 97 % of the variability among samples is explained. An evident separation is observed between MM and *hp3/B^{Sh}* lines. The latter is positioned in the negative part of dimension 1, and MM lines are in the positive part or close to 0, such as #25 and the WT. The variable 'a' holds significant weight in dimension 2 and signifies the intensity of the red color. It can be seen in the graph, where the MM lines exhibit a higher value of this parameter compared to the *hp3/B^{Sh}* lines, as the MM fruits present a more intense red color in comparison to the *hp3/B^{Sh}* fruits. Conversely, the *hp3/B^{Sh}* lines, with a more yellow-orange color, have a higher value of 'b' than the MM lines. Additionally, we have the parameters ‘C’, which indicates saturation, and ‘H’, defined as a color wheel with red-purple at an angle of 0°, yellow at 90°, bluish-green at 180°, and blue at 270°. Lines #1, #3, and #12 present higher values of ’H’ than the MM lines, explaining the more yellowish hue of the fruits.

In Figure 8b, all *hp3/B^{Sh}* fruits at br+10 are represented, the first dimension clearly separates two *hp3/B^{Sh}* lines containing *GjCCD4a* (#1 and #3) from the rest; these lines show lower values in the ‘a’ variable, indicating that the fruit exhibits a less red colour compared to the others. Additionally, the values of ‘C’ and ‘b’ in these two lines are also lower, resulting in fruits that are slightly more subdued and yellowish compared to the rest. The WT is separated from all lines, but is closer to #12, indicating that the color difference between these two are less.

Lastly, in Figure 8c, all MM fruits at br+10 are represented. All lines containing only *GjCCD4a* are in the positive part of the dimension 1, except for #34. The variables exerting a greater influence in this dimension are L, H, and b, with the values of these lines being lower than those containing the double transgenes. Among the lines containing *GjCCD4a*, sample #3 exhibits the highest value of parameter 'a,' resulting in a fruit that is redder than the others. In contrast, those containing the double transgene have a lower 'a' value and a higher 'b' value, as the fruit displays a more yellowish hue compared to lines with only *GjCCD4a*. Line #34 deviates from this trend. Considering color saturation, it is higher in lines with the double transgene, causing the fruits to display more vivid yellow tones than those containing only *GjCCD4a*, which have a redder and more subdued color.

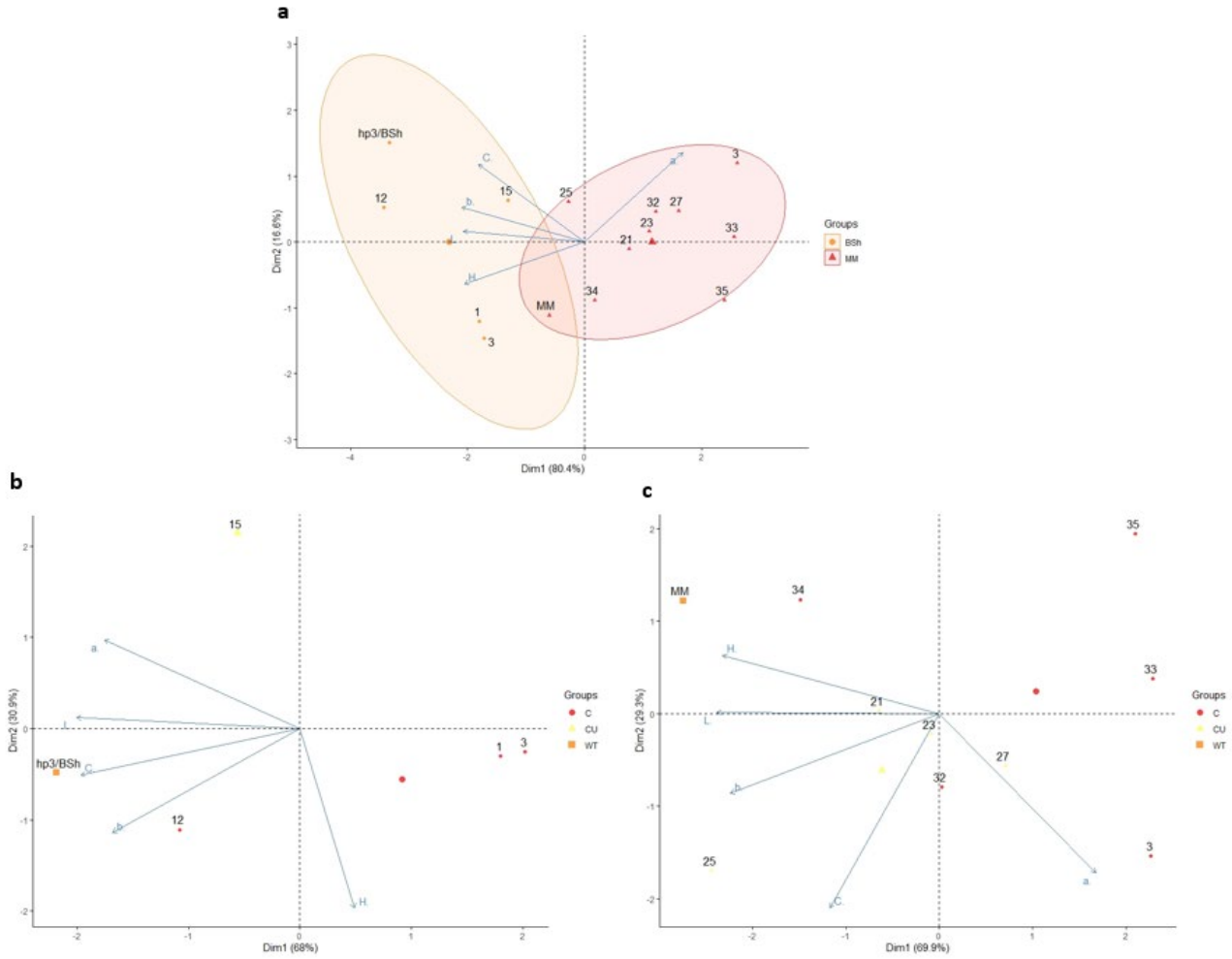

Figure 8. PCAs based on tomato fruit colour parameters. a) fruits at br+10 of all lines, also including WT of both *hp3/B^{Sh}* and MM, separated by background; b) fruits at br+10 of *hp3/B^{Sh}* lines, separated by transgene; c) fruits at br+10 of MM lines, separated by transgene. MM and *hp3/B^{Sh}* indicate WT. C, *GjCCD4a*; CU, *GjCCD4a-CsUGT91P3*; Dim, dimension.

Table 2. Contribution of the variables in the dimensions represented in the PCAs in Figure 8.

	Figura 8a		**Figura 8b**		**Figura 8c**	
	Dim.1	Dim.2	Dim.1	Dim.2	Dim.1	Dim.2
L*	22.48	0.69	28.60	0.22	27.97	0.00
a*	14.89	46.81	21.97	14.78	13.89	34.73
b*	23.12	7.12	20.16	20.26	24.75	8.69
H*	22.19	10.21	1.70	60.69	26.59	4.69
C*	17.30	35.14	27.55	4.02	6.78	51.87

Expression analysis of the transgenes

RNA extraction was carried out from the validated transgenic lines to ascertain the expression patterns of the input transgenes. Subsequently, cDNA was synthesized from the RNA, and qRT-PCR analysis was

conducted to assess the relative levels of gene expression among the lines. The primers used are detailed in Supplementary Material Table 3.

At br+5, line #33 showed the highest expression of *GjCCD4a* (0.5722 vs. actin), followed by line #21 (0.4518 vs. actin). The line with the lowest expression of *GjCCD4a* was #35 (0.0731 vs. actin). The only measured *hp3/B^{Sh}* line at br+5 was #15 (0.2838 vs. actin), lower than the expression in MM lines #3, #32, #33, and #21. Fruits at br+5 could not be collected from *hp3/B^{Sh}* lines #23, #1, #3, and #12.

At br+10, *hp3/B^{Sh}* line #1 displayed the highest expression in fruits (0.4225 vs. actin), followed by #23 (0.3671 vs. actin). In *hp3/B^{Sh}* lines, #3 and #12 exhibited lower expression values than #1 and #15. The line with the lowest expression of *GjCCD4a* was #34 (Figure 9a).

For the lines where fruits could be collected at both br+5 and br+10, *GjCCD4a* expression was generally lower in fruits at br+10 than at br+5, except for line #25.

The highest expression of *CsUGT91P3* at br+5 was in #21 (3.9824 vs. actin), followed by #27 (3.3012 vs. actin). Like *GjCCD4a*, *CsUGT91P3* expression is lower at br+10 than in br+5, with line #25 exhibiting the lowest expression (0.6454 vs. actin). The expression in other MM lines was similar. *CsUGT91P3* expression in *hp3/B^{Sh}* was extremely low compared to MM lines, both at br+5 and br+10 (< 0.02 vs. actin) (Figure 9b).

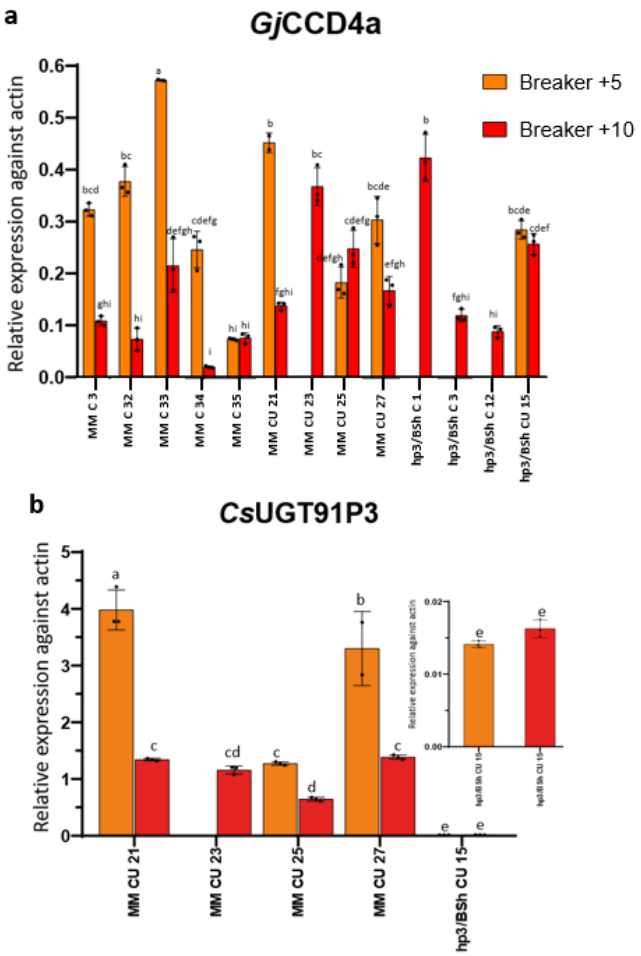

Figure 9. Relative expression of *GjCCD4a* (a) and *CsUGT91P3* (b) (normalized to actin) in the transgenic tomato lines. ANOVA and subsequent post hoc Tuckey were performed to see significative differences (α< 0.05) and group the lines.

Expression analysis of some carotenogenic genes

The expression of key genes in the carotenoid and MEP pathways was investigated to see if the introduction of the *GjCCD4a* that directs part of the carotenoids to the synthesis of apocarotenoids had any effect on these pathways and/or their regulation (Figure 10). The log2FC $2^{-\Delta\Delta Ct}$ relative to MM WT was calculated and the expression levels of the targeted genes in the br+5 samples were compared with MM WT br+5, and the br+10 samples were compared with MM br+10 samples.

Firstly, we examined the expression of the initial two genes in the MEP pathway, DXS and DXR (Figure 10a and 10b). The highest expression of DXS is observed in line #33 at br+5 (log2FC 2.7146). The subsequent lines showing higher expression at br+5 include #3, #35, and #27, all belonging to the MM group.

At br+10, the highest expression of DXS is noticed in line #15 *hp3/B^{Sh}* (2.1724 times higher than MM WT), followed by the WT of *hp3/B^{Sh}*. The only lines showing a downregulation relative to MM WT at br+10 are #32, #34, #21 in MM, and #12 in *hp3/B^{Sh}*, all at br+10.

Regarding DXR gene, we detect that the expression in all lines at br+5 was not relevant in comparing with MM WT. Only in MM #32 and *hp3/B^{Sh}* #15 lines at br+5 were upregulated, being 5.6-fold times higher than MM in the latter one. In br+10, the expression of DXR was generally downregulated in most lines, except #35, #25, #1, #3, #12, that exhibits a log2FC close to 0. The most significant downregulation od DXR was found in line #34, with a log2FC close to 3.

Summarizing, at br+5 DXS expression was in general upregulated in br+5, or maintained in some lines, in comparison with MM WT, suggesting that an increase in the MEP pathway occurred during this ripening stage. This could be provoked for an increased need of precursors for the carotenoid pathway as carotenoids are metabolized to apocarotenoids in our engineered fruit. Since DXS is the key enzyme in this pathway, it is regulated for more factors. However, the next biosynthesis step mediated by DXR does not show any clear increase in fruits at the same stage, rather being downregulated in the lines engineered only the *Gj*CCD4a.

Secondly, we study the effect on the key gene in the carotenoid pathway, PSY. The expression of isoforms 1 and 2 of PSY was analyzed (Figure 10c and 10d). PSY1 was mainly expressed in the fruit, while PSY2 was expressed in green tissues [14]. Looking at the expression of both genes, PSY1 was upregulated in most lines at br+5, except in #32, #34 and #21 that did not show relevant changes respect to MM WT. The highest expression was found in #33 (log2FC > 2), followed by #27 and #3, all MM lines. Studying the expression of PSY2 at br+5, no relevant up or downregulation was found in most lines. Only #3 and #33 lines showed two-fold higher upregulation comparing with MM WT.

Considering br+10, in PSY1, we noticed higher expression in lines #35, #23, and *hp3/B^{Sh}* WT. It seems that PSY1 were upregulated in early ripening stage when precursors are still needed to produce more complex carotenoids. Examining the expression of PSY2 at the same stage, all lines, except #15 and #21, did not show important changes in the gene expression in comparison with MM WT. Two upregulated lines contained both transgenes. Again, the conversion of carotenoids to apocarotenoids seem to activate carotenoid biosynthesis.

Expression of PSY1, in general, showed an upregulation, especially at br+5, that was not appreciated in PSY2 at the same stage. The same pattern was detectable at br+10, more lines were upregulated in contrast to PSY2, that only #15 had a log2FC > 1.

CYC-B1 and LCY-B1 enzymes are the responsible for producing β-carotene or α-carotene from lycopene. The CYC-B1 expression in *hp3/B^{Sh}* lines was significantly higher at both br+5 and br+10 compared to the MM lines, and this is attributed to the presence of the *B^{Sh}* mutation (Figure 10e). This mutation is known to result in an increased expression of this gene, leading to a substantial accumulation of β-carotene. [23]. #12 showed the highest expression with a log2FC value close to 6. Regarding the MM lines, the one with the highest expression was #35 at br+10, followed by #21 and #25 at the same stage.

On the other hand, the highest increase on LCY-B1 expression (Figure 10f) was found in #25 at br+5, followed by #15. Furthermore, *hp3/B^{Sh}* WT and #3 were upregulated at br+10. Conversely, nearly all MM lines at br+10 displayed downregulation of LCY-B1, except for lines #21, #25, and #27. None of MM plants carrying only *GjCCD4a* showed any relevant upregulation o downregulation of LCY-B1.

To sum up with these two cyclase genes, all lines containing the *B^{Sh}* mutation increase CYC-B1 expression in the ripening fruit. Furthermore, in these lines have the LCY-B1 gene upregulated, leading, presumably to increase β-carotene accumulation or flux (to be determined). In MM engineered lines, some of the ones carrying both transgenes showed an upregulation of the cyclase, whereas most MM lines engineered with only *Gj*CCD4a, showed either similar expression or a downregulation of the CY genes at br+10.

The highest increase on BCH1 expression (Figure 10g) was in #15, with a log2FC value higher than two. Line #1 showed appreciable values of upregulation (log2FC value higher than 1), in contrast to #3, that displayed similar downregulated levels. Interestingly, BCH1 was downregulated in all MM engineered only *Gj*CCD4*a*, at higher extent in br+5, except #35, that has a log2FC close to 0.

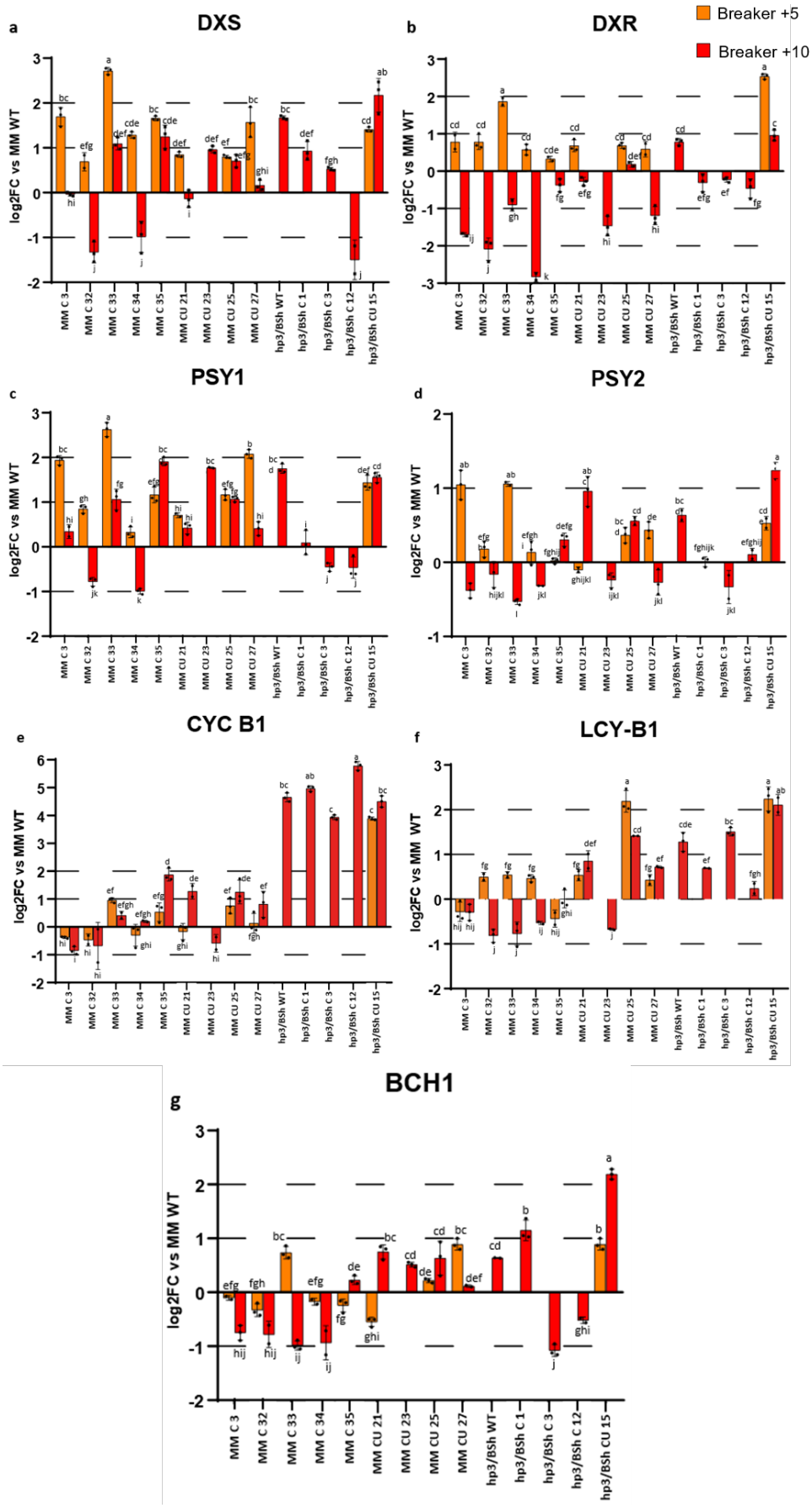

Figure 10. Log2FC vs MM WT of DXS (a) and DXR (b), PSY1 (c) and PSY2 (d), CYC-B1 (e) and LCY-B1 (f), and BCH1 (g). ANOVA and subsequent post hoc Tuckey were performed to see significative differences (α< 0.05) and group samples.

Saffron apocarotenoid analysis in transgenic tomato lines

After analyzed the expression of the transgenes and some genes of the carotenoid biosynthesis pathway, the last step is to study the saffron apocarotenoid content. Only the main saffron apocarotenoids where measured (Figure 11) while a more comprehensive apocarotenoid analysis will be conducted in the future. In both br+5 and br+10, the lines with the highest levels of saffron apocarotenoids were *hp3/B^{Sh}* lines #1 (5339.99 µg/g DW), #3 and #12 (4642.59 µg/g DW) carrying only *Gj*CCD4a, and #15 (4870.29 µg/g DW), carrying both *Gj*CCD4a and *Cs*UGT93P1. The pattern of crocin and picrocrocin accumulation was similar in the samples. Interestingly, crocin accumulation was higher than picrocrocin in all samples. However, further analysis of β-apocarotenoids (those originated from cyclated extremes of βcarotene) are needed as *Gj*CCD4a is capable of cleavage this substrate. Fruits in br+10 had a higher accumulation of saffron apocarotenoids in comparison with fruits in br+5, as expected for a metabolic end product based on a strategy driven by a ripening promoter. For instance, the mean of saffron apocarotenoid content of transgenic *hp3/B^{Sh}* lines is 2242.0949 µg/g DW, respect to 194.04 µg/g DW in MM in br+5 (11 times more). In br+10, the difference was even higher, 4478.25 µg/g DW in *hp3/B^{Sh}* lines and 290.65 µg/g DW in MM lines (15 times more).

The difference among lines containing C o CU vector was also noticed. At br+5, MM C accumulated 142.30 µg/g DW in comparison to MM CU 274.52 µg/g DW (almost the double). Similar difference was shown at br+10. This suggests that *Cs*UGT91P3 may be involved in synthesizing more stable glycosylated crocins than those produced by the endogenous UGTs of tomato.

Regarding MM lines, a significant difference can be seen between those lines that contain only *Gj*CCD4a and those with *Gj*CCD4a and *Cs*UGT93P1 at both ripening stages (Table 3). The lines with a higher apocarotenoid accumulation were #21 and #23 in br+10 fruits, which was slightly higher than those lines with only the *Gj*CCD4a. At br+10, this difference among lines with distinct transgenes cannot be observed in *hp3/B^{Sh}* lines. However, taking only the crocin and picrocrocin content separately, there is significant differences among *hp3/B^{Sh}* lines. In MM, we found that total saffron apocarotenoid content was significant different at br+5 and br+10, and between constructions (Table 3).

Table 3. Comparisons of total saffron apocarotenoids between lines containing one and two transgenes, and between ripening stage. Means and SDs of each group are indicated. t-test were made. $p < 0.05$.

Comparison of total saffron apocarotenoids	p-value	Mean group 1	SD group 1	Mean group 2	SD group 2
MM CU vs C Br+5	0.0077	274.52	110.08	142.30	75.51
MM CU vs C Br+10	0	394.21	63.62	201.89	115.50
MM Br+5 vs Br+10	0.0084	194.04	110.13	290.65	135.19
hp3/B^{Sh} CU vs C Br+10	0.1694	4870.29	110.85	4347.57	1026.93

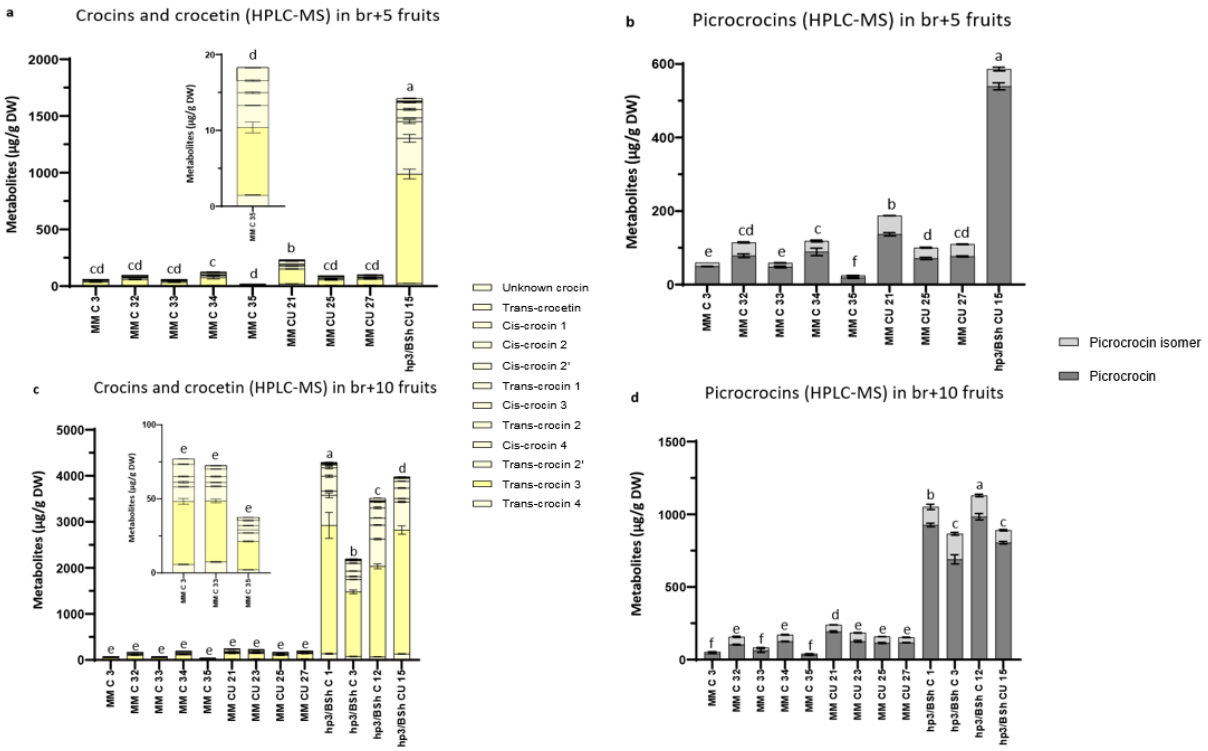

Figure 11. Absolut quantification of crocins and crocetin *(a and c*) and picrocrocins (b *and d*) in br+5 *and br+10* fruits. ANOVA and subsequent post hoc Tuckey were performed to see significative differences (α< 0.05) and group samples.

If we look at the glycosylation levels of crocins that we found in the analysis, the highest glycosylated crocins is four sugar residues (crocin 4). However, the most accumulated crocin was *trans*-crocin 3. Examining the content of these two crocins respect the total crocin content, at br+10, MM C lines showed only a 11.16 % of crocin 4 (*cis* and *trans*) was detected compared with the 13.48 % in MM CU. Regarding crocin 3 (*cis* and *trans*), similar differences was observed (64.64 % vs 66.99 %). In *hp3/B^{Sh}* lines, same pattern was detected. *hp3/B^{Sh}* C lines had a higher proportion compared with the CU lines (7.43 % vs 5.12 %). However, respect crocin 3, CU lines showed higher proportion (67.37 % vs 71.29 %). No t-test was performed to see significant differences.

Connecting the crocin content with the development of the lines and other aspects of the fruit phenotypes, our observations revealed that all lines in the mutant *hp3/B^{Sh}* background, which accumulate more crocins, experienced more challenging growth and yielded fewer fruits compared to the MM lines. These developmental issues may arise from a potential deficiency in ABA resulting from the *hp3* mutation+.

The weight of the fruits was measured to see any possible differences associated to our apocarotenoid engineering approach to the transgenic lines (Figure 12). The lines that exhibited the highest median fruit weights were MM *GjCCD4a* lines #3, #33, and #35 (34.63 g, 36.25 g, and 38.31 g, respectively), with values similar to the WT. Conversely, #32 and #34 showed median values similar to MM lines

expressing both transgenes. Line #27 had the lowest median value (9.98 g) among all lines, although it had the highest variance in fruit weight. The median and distribution among transgenic *hp3/B*^{Sh} lines were similar.

Precisely in these last lines was where the highest content of crocins and picrocrocin was detected. However, the median of the WT was higher (38.31 g) than the transgenic lines. This difference may be partly due to pleiotropic effects of the accumulation of apocarotenoids derived from the action of *Gj*CCD4a, although further studies are needed to investigate this approach more deeply. The absence of ABA because of *hp3* mutation is another crucial factor that may be involved in these observations. A similar trend was observed in the MM lines; those with a higher amount of crocins and picrocrocins were engineered with *Gj*CCD4a and *Cs*UGT91P3. These presented medians between 9-18 g, and both the MM lines, expressing only *Gj*CCD4a, and the WT lines have medians greater than 30 g (except #32 and #34). No t-test was performed to check if the differences between medians were significant.

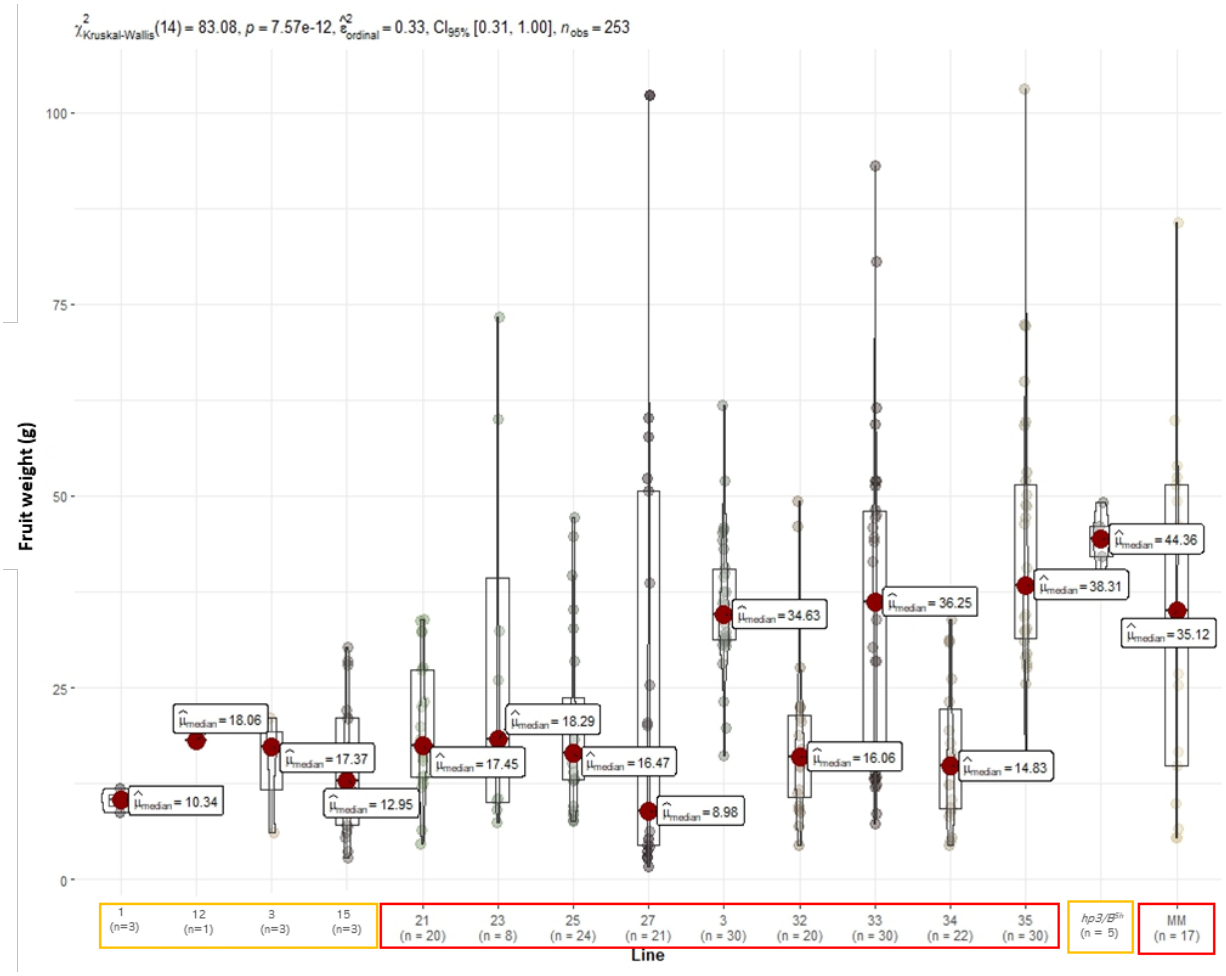

Figure 12. Fruit weight data from select transgenic lines were collected, and the median weight for each line is indicated. MM lines are represented by red boxes, while *hp3/B*^{Sh} lines are represented by orange boxes. MM WT and *hp3/B*^{Sh} WT are positioned on the right side of the graph.

Discussion and Future perspectives

This project is built upon the utilization of the tomato as a heterologous platform for producing saffron apocarotenoids, an achievement previously reached with the so-called Tomaffron [46], where the *Crocus sativus* (saffron) *Cs*CCD2L was expressed in the MM tomato cultivar [46]. In this work we explored an alternative way for producing saffron apocarotenoids in tomato fruits. To achieve this, another CCD, specifically the *Gardenia Gj*CCD4a has been introduced in tomato plants. *Gj*CCD4a is reported to utilize lycopene, β-carotene, and zeaxanthin as substrates [27]. To find out the best production platform as provide by different substrate combinations, transgenic lines expressing of *Gj*CCD4a were generated, for both the MM, which predominantly accumulates lycopene in the fruit, and for the double mutant *hp3/B*^{Sh}, which primarily accumulates β-carotene and also accumulates detectable levels of zeaxanthin in the fruit.

Following the implementation of the transformation protocol and the generation of transgenic lines, those confirmed by PCR were transferred to soil. Interestingly, there was a notable difference in the growth between the MM and *hp3/B*^{Sh} lines. The MM lines exhibited faster growth, and their fruits were harvested earlier than those of the *hp3/B*^{Sh} lines. Some confirmed transgenic plants of *hp3/B*^{Sh} transferred to soil exhibited defective growth, resulting in floral abortions or the production of non-harvestable fruits. These plants were excluded from the final analysis due to the lack of fruit material. This can be due to the *hp3* mutation impairs ZEP in the carotenogenesis pathway, leading an accumulation of zeaxanthin. This zeaxanthin cannot be converted in ABA, causing a deficient in the plant [23]. The role of ABA has been identified as pivotal in the development and numerous processes within the plant. For instance, current research is to explore how ABA may be involved in the maturation of non-climacteric fruits, such as tomato [52].

Regenerated *hp3/B*^{Sh} showed this growth problems. Fewer fruits could be collected compared to MM lines, even was not possible to collect at br+5, only in line #15. In addition to the impact of mutations in these plants, it may be that the content of crocin and picrocrocin also contributes to the defective development. However, more studies are needed to investigate the possible impact of these apocarotenoids on the plant.

Measuring the color of tomato fruits is a crucial and widely utilized parameter. During the ripening process, tomatoes undergo changes that alter their composition, including the synthesis of carotenoids. Additionally, color measurement is important in post-harvest stages for detecting pathogens such as fungi and is even employed as a target in breeding efforts [50], [53].

With these measurements, we made to establish an objective way to detect color changes measured from the outer surface of transgenic tomatoes during ripening that would indicate the presence of

crocins. A principal component analysis (PCA) was conducted to separate transgenic lines from the WT. In case to be such separation, this should be cause by the crocin accumulation and the colour change. Firstly, it is evident how the MM lines distinctly separate from the *hp3/B^{Sh}* lines. This was already known, given that the double mutant accumulates significantly more β-carotene, resulting in orange fruit instead of red. This is why the MM lines are close to the variable a* in the PCA, which defines the red color.

An attempt was made to establish a separation based on the expressed transgene/crocins accumulation. Regarding *hp3/B^{Sh}* lines, there appears to be some separation between the constructions. In lines #1 and #3, the variables a*, as well as H* or C*, do not seem to directly contribute to the red color of these fruits, as they are on the opposite side of the graph. Nevertheless, it would be interesting to measure the internal color of the fruit in the endocarp, as the typical color of crocins is predominantly observed in the internal part of the fruit. Similarly, more data on color measurements are needed to draw more robust conclusions.

Examining the color space of the MM lines, those expressing only *Gj*CCD4a do not seem to exhibit a clear pattern. However, those expressing the double transgene, appears to have a more uniform color, and what is more interesting, they are clearly separated from the control fruits. Nevertheless, further analyses are necessary, similar to what is needed for the *hp3/B^{Sh}* lines.

The carotenoid biosynthetic pathway has been extensively studied and characterized over the years due to the significant commercial and industrial interest in these compounds [1].

Given that apocarotenoids, in this case, those from saffron (crocins, crocetin, picrocrocin, and safranal), arise from the catabolism of carotenoids, [40], it is crucial to observe how the key genes in the pathway behave in our transgenic lines.

The fact that there is higher expression of *Gj*CCD4a at br+5 indicates that the E8 promoter exhibits thee expect pattern of expression defined for the E8 gene (TomExpress), since the mRNA is translated into a protein and the protein has to reach the maximum activity rate, and the product is then accumulated even more at later stages. Interestingly, the *GjCCD4a* relative expression levels were lower when compared to those of *CsUGT91P3* driven by the same E8 promoter in the same lines. These could be due to different stabilities of the transcripts, a positional effect on the construct inserted or different efficiencies in the RT-PCR. On the other hand, variations in *GjCCD4a* expression across different lines may suggest inserting different number of copies of the T-DNA into the plant genome or insertion in regions with different accessibility for the transcriptional machinery. For instance, #1 line showed the highest expression of CCD4a and is the line with the highest content in crocins. Also, #23 MM line follows the same pattern, being the highest line, together with #21 in crocin

accumulation. Conducting qPRC, Southern blot analysis, insertion cloning etc, would be necessary to verify the presence of multiple copies in any of the lines.

Comparing the saffron apocarotenoid content between ripening stages in MM lines, we find that the accumulation in br+10 is around 1.5 times higher than in br+5 fruits (290.65 vs 194.04 µg/g DW). This value could be assumed since the carotenoid precursors should be accumulated in advanced ripening stages. However, carotenoid analysis should be performed to confirm all these data. Comparing between lines with different constructions in MM, we observed that the accumulation of crocins is almost two times higher in those with both transgenes (172.10 vs 334.36 µg/g DW).

Glycosylation is a crucial process for the transport and storage of crocins [41]. UGTs seem to play an important role in determining the nature of crocins and their derivatives that can accumulate in a plant. For instance, it was observed that infiltrating *Cs*CCD2L along with a virus into *N. benthamiana* leaves resulted in a lower quantity of highly glycosylated apocarotenoids than when *Cs*CCD2L was inoculated without the virus. The virus appears to saturate ALDH and UGTs, preventing the production of highly glycosylated crocins [51]. It is known that endogenous ALDHs and UGTs in tomato fruit are promiscuous and can glycosylate crocetin to different crocins, similarly to what *Crocus* enzymes do in *Crocus* stigmas [46].

The hypothesis of employing *Cs*UGT91P3 is based on the possibility that it may synthesize more highly glycosylated crocins than could be produced by the endogenous UGTs in tomato. However, only crocins with glycosylated from one to four residues were detected, a similar pattern as it was found in Tomaffron [46]. In *N. benthamiana* leaves, a total amount of 30.5 µg/g DW of 1-4 glycosylated crocins were quantified, expressing *Cs*CCD2L and a different UGT, *Cs*UGT709G1 [45]. This quantity is notably lower in comparison whit the obtained in this project, 334.36 µg/g DW in MM lines and 3556.19 µg/g DW in *hp3/B^{Sh}* lines, both expressing *Cs*UGT91P3. Despite this, in the MM lines, a two-fold increase was observed between those with and without the *Cs*UGT91P3.

A difference does exist between the MM and *hp3/B^{Sh}* lines, suggesting that *Gj*CCD4a has a stronger preference for cyclic carotenoids derived from β-carotene as a substrate to yield crocins and derivatives because β-carotene content is higher in *hp3/B^{Sh}* plants. This is due to the *hp3* and *B^{Sh}* mutations, which impair ZEP and increase the expression of CYC-B, respectively, leading to an increase in β-carotene levels. The presence of *Cs*UGT93P1 does not appear to be a major factor in the accumulation of crocins, crocetin, and picrocrocin in *hp3/B^{Sh}*. Carotenoid quantification would be necessary to study the metabolite pattern when *Gj*CCD4a with/without the *Cs*UGT91P3. Also, apocarotenoids derived from the extreme of lycopene, β-carotene and zeaxanthin should be analyzed to elucidate the action of *Gj*CCD4a in the substrates.

The production of saffron apocarotenoids has been achieved in several biotech platforms, from microorganisms to plants (Table 1), due to advances in synthetic biology and metabolic engineering [44]. We find promising outcomes when comparing the results obtained in this project with those of previous studies. The transient agroinfiltration of *Gj*CCD4a into *N. benthamiana* leaves allowed the accumulation of 1.63 mg/g DW of crocins, a quantity twice as high as that obtained with the agroinfiltration of *Cs*CCD2L (0.67 mg/g DW) [27]. In this case, the accumulation of crocins obtained in tomato *hp3/B^{Sh}* was approximately 2.6 times higher than that achieved with *Gj*CCD4a in *N. benthamiana*, and in a stable manner.

In comparison with other heterologous productions, the results remain quite promising. For instance, in *S. tuberosum*, 1.16 mg/g DW of saffron apocarotenoids were obtained using *Cs*CCD2L and two UGTs. The amount obtained in this work was approximately 4.6 times higher than that obtained in potato [47]. However, the most productive system for accumulating crocins remains Tomaffron (16.9 mg/g DW) [46], with the 5.34 mg/g DW accumulated in the #1 *hp3/B^{Sh}* line falling short in comparison. Those high producing lines however were very difficult to grow and propagate what would set a limit of 5 mg/g DW of ripe fruit for a viable tomato-based platform. Our approach may also produce additional levels of other cyclic or linear apocarotenoids.

To conclude, the future prospects for this line of work involve obtaining the T1 generation of the most productive lines, both in MM and *hp3/B^{Sh}* backgrounds, and conducting relevant transcriptomic and metabolomic analyses, and viability assessment of the derived apocarotenoid production platforms. Furthermore, more in-depth metabolomic analyses will be undertaken to study the carotenoid content in fruits accumulating crocins. This will allow the identification of preferred substrates for *Gj*CCD4a in the fruit context.

Conclusions

From this project, we can conclude that:

- *Gj*CCD4a can be used as a biotechnological tool capable of producing saffron apocarotenoids in tomato fruits under the control of the E8 fruit-specific promoter in both MM and *hp3/B*^{Sh} genetic backgrounds.

- The expression of *Gj*CCD4a in tomato fruit produces a higher quantity of crocins (15-fold) in *hp3/B*^{Sh} lines compared to MM lines.

- *Cs*UGT91P3 leads a higher crocin accumulation in the *Gj*CCD4a engineered MM lines.

References

[1] M. Rodriguez-Concepcion *et al.*, "A global perspective on carotenoids: Metabolism, biotechnology, and benefits for nutrition and health," *Progress in Lipid Research*, vol. 70. Elsevier Ltd, pp. 62–93, Apr. 01, 2018. doi: 10.1016/j.plipres.2018.04.004.

[2] Y. Jiao, L. Reuss, and Y. Wang, "β-Cryptoxanthin: Chemistry, Occurrence, and Potential Health Benefits," *Current Pharmacology Reports*, vol. 5, no. 1. Springer International Publishing, pp. 20–34, Feb. 15, 2019. doi: 10.1007/s40495-019-00168-7.

[3] H. Hashimoto, C. Uragami, and R. J. Cogdell, "Carotenoids and photosynthesis," *Subcell Biochem*, vol. 79, pp. 111–139, Aug. 2016, doi: 10.1007/978-3-319-39126-7_4.

[4] L. Stanley and Y. W. Yuan, "Transcriptional Regulation of Carotenoid Biosynthesis in Plants: So Many Regulators, So Little Consensus," *Frontiers in Plant Science*, vol. 10. Frontiers Media S.A., Aug. 09, 2019. doi: 10.3389/fpls.2019.01017.

[5] F. Matthäus, M. Ketelhot, M. Gatter, and G. Barth, "Production of lycopene in the non-carotenoid-producing yeast Yarrowia lipolytica," *Appl Environ Microbiol*, vol. 80, no. 5, pp. 1660–1669, Mar. 2014, doi: 10.1128/AEM.03167-13.

[6] D. Ribeiro, M. Freitas, A. M. S. Silva, F. Carvalho, and E. Fernandes, "Antioxidant and pro-oxidant activities of carotenoids and their oxidation products," *Food and Chemical Toxicology*, vol. 120. Elsevier Ltd, pp. 681–699, Oct. 01, 2018. doi: 10.1016/j.fct.2018.07.060.

[7] I. Jaswir, D. Noviendri, R. F. Hasrini, and F. Octavianti, "Carotenoids: Sources, medicinal properties and their application in food and nutraceutical industry," *J Med Plant Res*, vol. 5, no. 33, pp. 7119–7131, Dec. 2011, doi: 10.5897/JMPRx11.011.

[8] A. Kulawik, J. Cielecka-Piontek, and P. Zalewski, "The Importance of Antioxidant Activity for the Health-Promoting Effect of Lycopene," *Nutrients*, vol. 15, no. 17. Multidisciplinary Digital Publishing Institute (MDPI), Sep. 01, 2023. doi: 10.3390/nu15173821.

[9] J. A. Paine *et al.*, "Improving the nutritional value of Golden Rice through increased pro-vitamin A content," *Nat Biotechnol*, vol. 23, no. 4, pp. 482–487, 2005, doi: 10.1038/nbt1082.

[10] F. Tuj Johra, A. Kumar Bepari, A. Tabassum Bristy, and H. Mahmud Reza, "A mechanistic review of β-carotene, lutein, and zeaxanthin in eye health and disease," *Antioxidants*, vol. 9, no. 11. MDPI, pp. 1–21, Nov. 01, 2020. doi: 10.3390/antiox9111046.

[11] U. Karniel, A. Koch, D. Zamir, and J. Hirschberg, "Development of zeaxanthin-rich tomato fruit through genetic manipulations of carotenoid biosynthesis," *Plant Biotechnol J*, vol. 18, no. 11, pp. 2292–2303, Nov. 2020, doi: 10.1111/pbi.13387.

[12] L. D'Andrea, "Molecular regulation of carotenoid biosynthesis in tomato fruits. New biotechnological strategies," Universitat Autónoma de Barcelona, Barcelona, 2016.

[13] T. Sun, S. Rao, X. Zhou, and L. Li, "Plant carotenoids: recent advances and future perspectives," *Molecular Horticulture*, vol. 2, no. 1. BioMed Central Ltd, Dec. 01, 2022. doi: 10.1186/s43897-022-00023-2.

[14] H. Cao *et al.*, "A neighboring aromatic-aromatic amino acid combination governs activity divergence between tomato phytoene synthases," *Plant Physiol*, vol. 180, no. 4, pp. 1988–2003, Aug. 2019, doi: 10.1104/pp.19.00384.

[15] C. Rosati, G. Diretto, and G. Giuliano, "Biosynthesis and engineering of carotenoids and apocarotenoids in plants 151 Biosynthesis and Engineering of Carotenoids and Apocarotenoids in Plants: State of the Art and Future Prospects," 2009.

[16] T. Chattopadhyay, P. Hazra, S. Akhtar, D. Maurya, A. Mukherjee, and S. Roy, "Skin colour, carotenogenesis and chlorophyll degradation mutant alleles: genetic orchestration behind the fruit colour variation in tomato," *Plant Cell Reports*, vol. 40, no. 5. Springer Science and Business Media Deutschland GmbH, pp. 767–782, May 01, 2021. doi: 10.1007/s00299-020-02650-9.

[17] R. Daphnee, N. Tchonkouang, M. Dulce, C. Antunes, M. Margarida, and C. Vieira, "Potential of Carotenoids from Fresh Tomatoes and Their Availability in Processed Tomato-Based Products," in *Carotenoids - New Perspectives and Application*, 2022. [Online]. Available: www.intechopen.com

[18] P. D. Fraser *et al.*, "Manipulation of phytoene levels in tomato fruit: Effects on isoprenoids, plastids, and intermediary metabolism," *Plant Cell*, vol. 19, no. 10, pp. 3194–3211, 2007, doi: 10.1105/tpc.106.049817.

[19] T. Isaacson, G. Ronen, D. Zamir, and J. Hirschberg, "Cloning of tangerine from tomato reveals a Carotenoid isomerase essential for the production of β-carotene and xanthophylls in plants," *Plant Cell*, vol. 14, no. 2, pp. 333–342, 2002, doi: 10.1105/tpc.010303.

[20] C. J. Orchard *et al.*, "Identification and assessment of alleles in the promoter of the Cyc-B gene that modulate levels of β-carotene in ripe tomato fruit," *Plant Genome*, vol. 14, no. 1, Mar. 2021, doi: 10.1002/tpg2.20085.

[21] H. V. Kilambi *et al.*, "Green-fruited Solanum habrochaites lacks fruit-specific carotenogenesis due to metabolic and structural blocks," *J Exp Bot*, vol. 68, no. 17, pp. 4803–4819, Aug. 2017, doi: 10.1093/jxb/erx288.

[22] M. Dalal, V. Chinnusamy, and K. C. Bansal, "Isolation and functional characterization of Lycopene β-cyclase (CYC-B) promoter from Solanum habrochaites," 2010. [Online]. Available: http://www.biomedcentral.com/1471-2229/10/61

[23] U. Karniel, A. Koch, D. Zamir, and J. Hirschberg, "Development of zeaxanthin-rich tomato fruit through genetic manipulations of carotenoid biosynthesis," *Plant Biotechnol J*, vol. 18, no. 11, pp. 2292–2303, Nov. 2020, doi: 10.1111/pbi.13387.

[24] G. Ronen, L. Carmel-Goren, D. Zamir, and J. Hirschberg, "An alternative pathway to-carotene formation in plant chromoplasts discovered by map-based cloning of Beta and old-gold color mutations in tomato," 2000. [Online]. Available: www.pnas.orgcgidoi10.1073pnas.190177497

[25] N. Galpaz, Q. Wang, N. Menda, D. Zamir, and J. Hirschberg, "Abscisic acid deficiency in the tomato mutant high-pigment 3 leading to increased plastid number and higher fruit lycopene content," *Plant Journal*, vol. 53, no. 5, pp. 717–730, Mar. 2008, doi: 10.1111/j.1365-313X.2007.03362.x.

[26] R. Azari *et al.*, "Light signaling genes and their manipulation towards modulation of phytonutrient content in tomato fruits," *Biotechnology Advances*, vol. 28, no. 1. pp. 108–118, Jan. 2010. doi: 10.1016/j.biotechadv.2009.10.003.

[27] X. Zheng *et al.*, "Gardenia carotenoid cleavage dioxygenase 4a is an efficient tool for biotechnological production of crocins in green and non-green plant tissues," *Plant Biotechnol J*, vol. 20, no. 11, pp. 2202–2216, Nov. 2022, doi: 10.1111/pbi.13901.

[28] H. Imtiaz, Y. Arif, P. Alam, and S. Hayat, "Apocarotenoids biosynthesis, signaling regulation, crosstalk with phytohormone, and its role in stress tolerance," *Environmental and Experimental Botany*, vol. 210. Elsevier B.V., Jun. 01, 2023. doi: 10.1016/j.envexpbot.2023.105337.

[29] O. Ahrazem *et al.*, "The carotenoid cleavage dioxygenase CCD2 catalysing the synthesis of crocetin in spring crocuses and saffron is a plastidial enzyme," *New Phytologist*, vol. 209, no. 2, pp. 650–663, Jan. 2016, doi: 10.1111/nph.13609.

[30] E. Nambara and A. Marion-Poll, "Abscisic acid biosynthesis and catabolism," *Annual Review of Plant Biology*, vol. 56. pp. 165–185, 2005. doi: 10.1146/annurev.arplant.56.032604.144046.

[31] X. Hou, J. Rivers, P. León, R. P. McQuinn, and B. J. Pogson, “Synthesis and Function of Apocarotenoid Signals in Plants,” *Trends in Plant Science*, vol. 21, no. 9. Elsevier Ltd, pp. 792–803, 2016. doi: 10.1016/j.tplants.2016.06.001.

[32] J. Y. Wang *et al.*, “The apocarotenoid metabolite zaxinone regulates growth and strigolactone biosynthesis in rice,” *Nat Commun*, vol. 10, no. 1, Dec. 2019, doi: 10.1038/s41467-019-08461-1.

[33] F. Li, X. Gong, Y. Liang, L. Peng, X. Han, and M. Wen, “Characteristics of a new carotenoid cleavage dioxygenase NtCCD10 derived from Nicotiana tabacum,” *Planta*, vol. 256, no. 5, Nov. 2022, doi: 10.1007/s00425-022-04013-y.

[34] S. A. Baba and N. Ashraf, “Carotenoid Cleavage Dioxygenases of Crocus sativus L.,” 2016, pp. 23–37. doi: 10.1007/978-981-10-1899-2_2.

[35] A. M. Sánchez and P. Winterhalter, “Carotenoid cleavage products in saffron (Crocus sativus L),” in *ACS Symposium Series*, American Chemical Society, 2013, pp. 45–63. doi: 10.1021/bk-2013-1134.ch005.

[36] M. Jamilena, A. López, E. Rakosy-Tican, and M. Kafi, “Monochromatic blue light enhances crocin and picrocrocin content by upregulating the expression of underlying biosynthetic pathway genes in saffron (Crocus sativus L.),” *Frontiers in Horticulture*, vol. 1, no. 96042, p. 96042, 2022.

[37] P. Winterhalter and M. Straubinger, “Saffron - Renewed interest in an ancient spice,” *Food Reviews International*, vol. 16, no. 1, pp. 39–59, 2000, doi: 10.1081/FRI-100100281.

[38] L. Gómez-Gómez *et al.*, “Engineering the production of crocins and picrocrocin in heterologous plant systems,” *Industrial Crops and Products*, vol. 194. Elsevier B.V., Apr. 01, 2023. doi: 10.1016/j.indcrop.2023.116283.

[39] O. C. Demurtas *et al.*, “Candidate enzymes for saffron crocin biosynthesis are localized in multiple cellular compartments,” *Plant Physiol*, vol. 177, no. 3, pp. 990–1006, Jun. 2018, doi: 10.1104/pp.17.01815.

[40] O. Ahrazem *et al.*, “Metabolic Engineering of Crocin Biosynthesis in Nicotiana Species,” *Front Plant Sci*, vol. 13, Mar. 2022, doi: 10.3389/fpls.2022.861140.

[41] A. J. López *et al.*, “A new glycosyltransferase enzyme from family 91, ugt91p3, is responsible for the final glucosylation step of crocins in saffron (Crocus sativus l.),” *Int J Mol Sci*, vol. 22, no. 16, Aug. 2021, doi: 10.3390/ijms22168815.

[42] L. Xie *et al.*, “Synthesis of Crocin I and Crocin II by Multigene Stacking in Nicotiana benthamiana,” *Int J Mol Sci*, vol. 24, no. 18, Sep. 2023, doi: 10.3390/ijms241814139.

[43] L. Morote *et al.*, “Verbascum species as a new source of saffron apocarotenoids and molecular tools for the biotechnological production of crocins and picrocrocin,” *Plant Journal*, 2023, doi: 10.1111/tpj.16589.

[44] T. Liu *et al.*, “Prospects and progress on crocin biosynthetic pathway and metabolic engineering,” *Computational and Structural Biotechnology Journal*, vol. 18. Elsevier B.V., pp. 3278–3286, Jan. 01, 2020. doi: 10.1016/j.csbj.2020.10.019.

[45] M. Martí *et al.*, “Efficient production of saffron crocins and picrocrocin in Nicotiana benthamiana using a virus-driven system,” *Metab Eng*, vol. 61, pp. 238–250, Sep. 2020, doi: 10.1016/j.ymben.2020.06.009.

[46] O. Ahrazem *et al.*, “Engineering high levels of saffron apocarotenoids in tomato,” *Hortic Res*, vol. 9, 2022, doi: 10.1093/hr/uhac074.

[47] L. Gómez Gómez *et al.*, “Fortification and bioaccessibility of saffron apocarotenoids in potato tubers,” *Front Nutr*, vol. 9, Nov. 2022, doi: 10.3389/fnut.2022.1045979.

[48] A. Sarrion-Perdigones *et al.*, “Goldenbraid 2.0: A comprehensive DNA assembly framework for plant synthetic biology,” *Plant Physiol*, vol. 162, no. 3, pp. 1618–1631, 2013, doi: 10.1104/pp.113.217661.

[49] P. Ellul, B. Garcia-Sogo, B. Pineda, G. Ríos, L. A. Roig, and V. Moreno, "The ploidy level of transgenic plants in Agrobacterium-mediated transformation of tomato cotyledons (Lycopersicon esculenturn L.Mili.) is genotype and procedure dependent," *Theoretical and Applied Genetics*, vol. 106, no. 2, pp. 231–238, Jan. 2003, doi: 10.1007/s00122-002-0928-y.

[50] D. S. Kasampalis, P. Tsouvaltzis, and A. S. Siomos, "Chlorophyll fluorescence, non-photochemical quenching and light harvesting complex as alternatives to color measurement, in classifying tomato fruit according to their maturity stage at harvest and in monitoring postharvest ripening during storage," *Postharvest Biol Technol*, vol. 161, Mar. 2020, doi: 10.1016/j.postharvbio.2019.111036.

[51] O. C. Demurtas *et al.*, "Production of Saffron Apocarotenoids in Nicotiana benthamiana Plants Genome-Edited to Accumulate Zeaxanthin Precursor," *Metabolites*, vol. 13, no. 6, Jun. 2023, doi: 10.3390/metabo13060729.

[52] B. J. Li, D. Grierson, Y. Shi, and K. S. Chen, "Roles of abscisic acid in regulating ripening and quality of strawberry, a model non-climacteric fruit," *Horticulture Research*, vol. 9. Oxford University Press, 2022. doi: 10.1093/hr/uhac089.

[53] V. Thole *et al.*, "Analysis of Tomato Post-Harvest Properties: Fruit Color, Shelf Life, and Fungal Susceptibility," *Curr Protoc Plant Biol*, vol. 5, no. 2, Jun. 2020, doi: 10.1002/cppb.20108.

[54] Y. Wei *et al.*, "A Comprehensive Analysis of Carotenoid Cleavage Dioxygenases Genes in Solanum Lycopersicum," *Plant Mol Biol Report*, vol. 34, no. 2, pp. 512–523, Apr. 2016, doi: 10.1007/s11105-015-0943-1.

Supplementary Material

Supplementary Table 1. Genes and accession numbers used to construct the phylogenetic tree. S. lycopersicum Gene IDs were extracted from [54] and can be consulted in https://solgenomics.net/.

Gene	Accession number
CsCCD1	UHY14103.1
CsCCD2L	ACD62475.1
CsCCD4a	ACD62476.1
CsCCD4b	ACD62476.1
CsCCD4c	AEO50759.1
CsCCD7	AIF27228.1
CsCCD8a	AIF27229.1
CsCCD8b	AIF27230.1
CaCCD2	AKN09909.1
BoCCD1-3	AMJ39497.1
BoCCD4-3	AMJ39501.1
BdCCD4.1	APU54674.1
BdCCD4.3	APU54676.1
GjCCD4a	ARU08109.1
AtCCD1	AEE80498.1
AtCCD7	AEC10494.2
AtCCD8	AEE86121.1
SlCCD1a	Solyc01g087250 (Gene ID)
SlCCD1b	Solyc01g087260 (Gene ID)
SlCCD4a	Solyc08g075480 (Gene ID)
SlCCD4b	Solyc08g075490 (Gene ID)
SlCCD7	ACY39883.1
SlCCD8	Solyc08g066650 (Gene ID)

Supplementary Table 2. GB parts used and generated.

ID	Construct
GB0015	pDGB3_alpha1 (a1)
GB0017	pDGB3_alpha2 (a2)
GB0019	pDGBb3_omega1 (o1)

GB0021	pDGB3_omega2 (o2)
GB0226	pDGB_Tnos:NptII:Pnos
GB0307	pUPD2
GB0914	pUPD2_PromE8
GB4659	pUPD2_CsUGTgg
GB4794	pUPD2_GjCCD4a
GB4796	a2_PE8:GjCCD4a:T35S
GB4797	o1_PE8:GjCCD4a:T35S_nptII
GB4844	a1_PE8:UGTgg:T35S
GB4860	o2_PE8:UGTgg:T35S
GB4861	a1_PE8:CCD4a_PE8:UGTgg_nptII

Supplementary Table 3. Oligonucleotides used.

ID	**Sequence**	**Use**
GjCCD4a-Seq	Forward: GCTCACCAAATTCTTCAATGCAC Reverse: TGCTGTCAATGCTTGGGATG	Sequencing of *Gj*CCD4a
GjCCD4a-Gen	Forward: CAACCTCCATGCCACTTGTC Reverse: TGATTGCGGCTTGGGATTGG	Genotyping of transgenic lines with *GjCCD4a*. Forward sequence is from E8 promotor.
CsUGT91P3-Gen	Forward: CAACCTCCATGCCACTTGTC Reverse: GAGGTACTGGAGGTTTGCCG	Genotyping of transgenic lines with *CsUGT91P3*. Forward sequence is from E8 promotor.
GjCCD4a-RT	Forward: ATCCCAAGCCGCAATCATCA Reverse: TTCCACCACCTCACATTCGG	Amplification for RT-qPCR.
CsUGT91P3-RT	Forward: TAGGCCTACTGCTGCCTACT Reverse: GCAGGATCTCGGTATCGCTC	Amplification for RT-qPCR.
Actin-2-RT	Forward: CATTGTGCTCAGTGGTGGTTC Reverse: TCTGCTGGAAGGTGCTAAGTG	Amplification for RT-qPCR.
Sl_DXR-RT	Forward: GCAGTGGGGCATTTGCTAAG Reverse: ACTTGTCCGGATTCTCAGCG	Amplification for RT-qPCR.
Sl_DXS-RT	Forward: TCAAAGACTGGGGGTCACCT Reverse:	Amplification for RT-qPCR.

	CCGGTGCCAAAGCAATCATA	
Sl_PSY1-RT	Forward: GTCGAAACGATGGCAGTTGG Reverse: CGTTGTTCGGGCGTTTGTAA	Amplification for RT-qPCR.
Sl_PSY2-RT	Forward: GTTGATATTCAGCCATTCAGAGAT Reverse: TTCAGGTGCAATGCCCATAA	Amplification for RT-qPCR.
Sl_BCH1-RT	Forward: GCCCAAAACCTACTTCGACA Reverse: CGCCAAGCGAGTAGCTAAGAT	Amplification for RT-qPCR.
Sl_CycB-RT	Forward: GTTATTGAGGAAGAGAAATGTGTGAT Reverse: TCCCACCAATAGCCATAACATTTT	Amplification for RT-qPCR.
Sl_LCYb1-RT	Forward: TGGATCTTGCTGTGGTTGGT Reverse: TAGCCTCAAATTCATCCACCCAA	Amplification for RT-qPCR.

Supplementary Table 4. Media culture for *Agrobacterium*. Amounts calculated for 1 L.

COMPOUND	SOC	MGL	TY	LB
Tryptone	20 g	5 g	5 g	10 g
Yeast extract	5 g	2.5 g	3 g	5 g
NaCl	10 mM	5 g		10 g
KCl	2.5 mM			
$MgCl_2$	10 mM			
Glucose	20 mM			
Mannitol		5 g		
Glutamic Ac.		1.02 g		
K_2HPO_4		252 mg		
$MgSO_4 \cdot 7H_2O$	10 mM	1 ml	1 ml	
Biotine		1 mg		
pH	pH 7	pH 5.6		
Acetosyringone		2 ml		
Kanamycin/Spectinomycin	50 mg	50 mg		
Rifampicin	50 mg			

Streptomycin	50 mg			

Supplementary Table 5. CTAB buffer components.

Extraction buffer (EB) – (without CTAB) for 250 ml		**CTAB buffer**	
NaCl 5M	70 ml	CTAB	1 g/50 ml EB
EDTA 0.5M	10 ml	β-mercaptoethanol	12 µl/600 µl EB
Tris-HCl pH 8 0.5M	50 ml	RNAse	1,6 µl/ml EB

Supplementary Table 6. Media used in tomato transformation. Amounts calculated for 1 L.

COMPOUND	**GM**	**CC**	**IM-1**	**IM-2**	**EM**	**RM**
MS including vitamins and MES buffer	2.5 g	4.9 g	4.9 g	4.9 g	4.9 g	2.5 g
Sucrose	15 g					
Glucose		20 g	20 g	20 g	20 g	20 g
Phyto Agar	10 g	10 g	10 g	10 g	10 g	10 g
	pH adjusted to 5.6-5.8 with KOH and autoclave 15-20’ at 121 ºC					
3-indolyacetic acid (1 mg/ml)		1 mg	1 mg	0.1 mg		0.2 mg
Trans-Zeatin (0.75 mg/ml)		0.75 mg	0.75 mg	0.75 mg	0.1 mg	
Acetosyringone (100 mM)		2 mL				
Carbenicillin (200 mg/ml)			400 mg	400 mg	400 mg	400 mg
Timentin (150 mg/ml)			150 mg	150 mg		
Kanamycin (100 mg/ml)			100 mg	100 mg	100 mg	100 mg

GM: Germination medium; CC: Cocultivation medium; IM: Induction medium; EM: Elongation medium; RM: Rooting medium.